



HAL
open science

Natural Denudation Versus Anthropogenically Accelerated Erosion in Central Brazil: A Confrontation of Time and Space Scales

Lionel L Siame, Lucas Espíndola Rosa, Luis Felipe Soares Cherem, José Guilherme de Oliveira, Olivier Evrard, Houda Barhoumi, Laëtitia Leanni, Adrien Duvivier, Pierre-henri Blard, Didier L Bourlès, et al.

► **To cite this version:**

Lionel L Siame, Lucas Espíndola Rosa, Luis Felipe Soares Cherem, José Guilherme de Oliveira, Olivier Evrard, et al. Natural Denudation Versus Anthropogenically Accelerated Erosion in Central Brazil: A Confrontation of Time and Space Scales. *Earth's Future*, 2023, 11 (8), pp.e2022EF003297. 10.1029/2022ef003297 . hal-04180633

HAL Id: hal-04180633

<https://hal.science/hal-04180633v1>

Submitted on 13 Aug 2023

HAL is a multi-disciplinary open access archive for the deposit and dissemination of scientific research documents, whether they are published or not. The documents may come from teaching and research institutions in France or abroad, or from public or private research centers.

L'archive ouverte pluridisciplinaire **HAL**, est destinée au dépôt et à la diffusion de documents scientifiques de niveau recherche, publiés ou non, émanant des établissements d'enseignement et de recherche français ou étrangers, des laboratoires publics ou privés.



Distributed under a Creative Commons Attribution 4.0 International License

Earth's Future

RESEARCH ARTICLE

10.1029/2022EF003297

†Deceased 1 March 2021

Key Points:

- Land degradation from increased continental erosion is a worldwide, systemic phenomenon due to human activities and climate change
- Isotopic methods allow comparing rates of preanthropogenic denudation to human-accelerated erosion
- Anthropogenically disturbed land surfaces in Brasília suffer from erosion rates 100 times higher than natural geomorphic process rates

Correspondence to:

L. L. Siame,
siame@cerege.fr

Citation:

Siame, L. L., Espíndola Rosa, L., Soares Cherem, L. F., de Oliveira, J. G., Evrard, O., Barhoumi, H., et al. (2023). Natural denudation versus anthropogenically accelerated erosion in Central Brazil: A confrontation of time and space scales. *Earth's Future*, 11, e2022EF003297. <https://doi.org/10.1029/2022EF003297>

Received 28 OCT 2022

Accepted 15 JUL 2023

Author Contributions:

Conceptualization: Lionel L. Siame, Sophie Cornu

Data curation: Lionel L. Siame

Formal analysis: Lionel L. Siame, Lucas Espíndola Rosa, Luis Felipe Soares Cherem, José Guilherme de Oliveira, Olivier Evrard, Houda Barhoumi, Laëtítia Leanni, Adrien Duvivier, Pierre-Henri Blard, ASTER Team

Funding acquisition: Lionel L. Siame, Sophie Cornu

Investigation: Lionel L. Siame

Methodology: Lionel L. Siame, Olivier Evrard, Didier L. Bourlès, Sophie Cornu

© 2023 The Authors. Earth's Future published by Wiley Periodicals LLC on behalf of American Geophysical Union. This is an open access article under the terms of the [Creative Commons Attribution-NonCommercial-NoDerivs License](https://creativecommons.org/licenses/by-nc-nd/4.0/), which permits use and distribution in any medium, provided the original work is properly cited, the use is non-commercial and no modifications or adaptations are made.

Natural Denudation Versus Anthropogenically Accelerated Erosion in Central Brazil: A Confrontation of Time and Space Scales

Lionel L. Siame¹ , Lucas Espíndola Rosa², Luis Felipe Soares Cherem³, José Guilherme de Oliveira⁴, Olivier Evrard⁵ , Houda Barhoumi¹, Laëtítia Leanni¹, Adrien Duvivier¹, Pierre-Henri Blard⁶, Didier L. Bourlès^{1,†}, ASTER Team¹, and Sophie Cornu¹

¹Aix Marseille Univ, CNRS, IRD, INRAE, CEREGE, Aix-en-Provence, France, ²Laboratory of Geomorphology, Pedology and Physical Geography (LABOGEF), Institute of Socio-Environmental Studies (IESA), Federal University of Goiás (UFG), Goiânia, Brazil, ³Department of Geography, Institute of Geosciences, Federal University of Minas Gerais, Belo Horizonte, Brazil, ⁴Department of Geography, Federal University of Paraná (UFPR), Curitiba, Brazil, ⁵Laboratoire des Sciences du Climat et de l'Environnement (LSCE/IPSL), Université Paris-Saclay, UMR 8212 (CEA-CNRS-UVSQ), Gif-sur-Yvette, France, ⁶CRPG, UMR 7358, CNRS, Université de Lorraine, Nancy, France

Abstract Land degradation resulting from increased continental surface erosion is a worldwide and systemic phenomenon due to unsustainable human activities. Already fragile, the intertropical zone is likely to be further affected by climate change like increased aridity, an aggravating factor of soil erosion and land degradation. A major challenge is thus to provide the necessary knowledge to not only deepen our understanding of the Earth's system and its critical thresholds but also to help achieving sustainability. Understanding the factors that control the properties and processes of the critical zone, and especially what will be its responses to ongoing climate and land use changes, requires multidisciplinary efforts to tackle time scales that are compatible with morphogenesis and soil development as well as environmental disturbances of anthropogenic origin. Due to its prominent ecological importance, the Brazilian Cerrado biome is an ideal natural laboratory where to gauge the consequences of recent and intense agricultural activities on continental surface erosion. We focused on the region of Brasília where our approach allows confronting the temporal scales of long-lived and stable cosmogenic nuclides with that of short-lived radioactive isotopes, through a comparison of natural and anthropogenically disturbed land surfaces. Our results indicate that long-term, background denudation rates are lower than 10 mm Kyr⁻¹ whereas recent erosion rates due to human activities may reach rates at least 160 times higher, exceeding by far the sustainability of the soil resource.

Plain Language Summary Soil erosion is a global threat to the well-being of billions of people. With the looming environmental crisis, this systemic problem is likely to get worse, especially in the developing and emerging regions where many countries are also more vulnerable to environmental and socio-economic instabilities. If human activities do not change the erosional mechanisms themselves, they however strongly modify the speed, frequency, and intensity of the erosive processes. This study proposes an original combination of techniques, each of them being well recognized in their scientific community but rarely combined to the best of our knowledge. We focused on the region of Brasília, and the Cerrado savanna, which is sensitive not only because of the dire need of ecosystem conservation but also due to conflicts between preservation of natural spaces and development of human activities. Our study shows how a landscape in a geomorphic state of equilibrium, where denudation and soil formation rates are in balance, is perturbed by agricultural activities with erosion rates at least 160 times faster, jeopardizing the sustainability of the soil resource.

1. Introduction

Understanding and quantifying environmental changes and their potential impacts on resources and society is a major challenge of the 21st century (e.g., Steffen et al., 2018). Within this context, continental surfaces are key since their evolution results from the forcing of long-established internal (i.e., tectonics) and external (i.e., climate) processes that are in turn disturbed by much shorter-term, and faster processes of anthropogenic origin, driving natural equilibria out of balance (Figure 1).

Project Administration: Lionel L. Siame
Resources: Lionel L. Siame
Supervision: Lionel L. Siame
Validation: Lionel L. Siame, Luis Felipe Soares Cherem, Laëtítia Leanni, Adrien Duvivier, Pierre-Henri Blard
Visualization: Lionel L. Siame, Lucas Espíndola Rosa
Writing – original draft: Lionel L. Siame
Writing – review & editing: Lucas Espíndola Rosa, Luis Felipe Soares Cherem, Olivier Evrard, Pierre-Henri Blard, Sophie Cornu

If human imprints on global land is continuous since millennia (Ellis et al., 2021), it might be four times higher than previously estimated (Winkler et al., 2021). Because of expansion of croplands and pastures at the expense of natural lands, unsustainable agriculture and forestry practices, urbanization, as well as development of infrastructures and extractive industries, human activities accelerated soil erosion (Borrelli et al., 2017), and induced losses of biodiversity (Dirzo et al., 2014; Le Tourneau, 2019), which now severely threaten eco-systemic services as well as the well-being of billions of people worldwide (IPCC, 2019). Indeed, climate projections predict that nearly a third of the world lands dedicated to food crops and animal production could trespass, by the end of the 21st century, the current and favorable conditions that have been slowly established during the Holocene (Kummu et al., 2021).

All these environmental changes expose the soil mantle to increased pressures and commit human societies to a profound change in both their organization and their development trajectories (Euzen et al., 2017; Ferdinand, 2019). This problem is sharper in intertropical regions since they host amongst the poorest countries on the planet, which are also more vulnerable to environmental and socio-economic instabilities (e.g., Scholes et al., 2018). Assessing the future dynamics of continental surfaces in response to climate and land use changes is thus a major challenge not only to deepen our understanding of the Earth system and its critical thresholds but also to strengthen our capacity to cope with sustainability issues.

Over millennia to millions of years, landscape evolution is primarily controlled by climate modulations, phases of tectonic activity, as well as other factors such as lithology and faulting of the rocks exposed to erosional processes at the surface (Figure 1). The combination of these natural forcing factors is responsible for the complex, interconnected geomorphic, pedological, biological, and hydrological processes that contribute to build of a sustainable, though fragile, critical zone (e.g., Brantley et al., 2007).

Although it is widely acknowledged that human activities have significant impacts on landscapes, these effects occur at different time and spatial scales compared to natural processes (Ackermann et al., 2014). Indeed, if human activities do not change the erosional mechanisms themselves, they however strongly modify the speed, frequency, and intensity of the erosive processes (e.g., Vanacker et al., 2014, 2019). It remains a challenge to accurately measure the relative contributions of natural factors (climate, tectonics, etc.) and anthropogenic impacts that disrupt the normal functioning of the critical zone (Poesen, 2018; Ruddiman, 2013). In the last 20 years, research on this topic has been conducted on both continental (Kemp et al., 2020) and global (Covault et al., 2013; Meybeck & Vörösmarty, 2005) scales, using time series analysis of various environmental variables such as fluvial sedimentary and chemical fluxes, alluvial sediment accumulation, and the use of cosmogenic radionuclides to quantify the denudation of the surface at catchment scale.

The aim of this study is to measure the rates of natural processes, specifically denudation and surface lowering rates, which are responsible for landscape evolution in Central Brazil over the long-term trend (10^3 – 10^6 years) and compare them to rates of human-accelerated erosion in the surroundings of the Federal Capital of Brasília, over the last decades (Figure 2). To accomplish this goal, a multiproxy approach (meteoric and in situ produced cosmogenic nuclides, fallout radionuclides, RUSLE models) has been tailored to compare natural areas (Cerrado-covered plateau in the National Park of Brasília) with anthropogenically disturbed lands (deforested plateau outside the National Park of Brasília). This approach results from an interdisciplinary collaboration among scientists in the fields of geomorphology, pedology, geochemistry, and geography. The raw data set compiling all the analytical results used in the current study is available in this in-text data citation reference: Siame et al. (2023).

2. Brief Review of Natural Denudation and Human-Induced Erosion Rates

At global and deep-time (Phanerozoic) scales, denudation rates for continental surfaces range from 15 to 40 mm kyr⁻¹, as estimated from preserved volumes of sedimentary rocks on continental and oceanic crusts (Wilkinson, 2005). A possible increase to a value of ≈ 55 mm kyr⁻¹ has also been reported for the Pliocene (Wilkinson & McElroy, 2007), although it remains debated whether climate change at the end of the Cenozoic had an effective impact on global erosion rates (Herman & Champagnac, 2016; Norton & Schlunegger, 2017; Willenbring & Jerolmack, 2016). These rates represent the balance between plate tectonics and climate fluctuations over hundreds of millions of years. For decennial time scales, river sediment loads yield an annual net riverine flux of all erosion and weathering products to the global ocean of about 21 Gt (Ludwig et al., 1996; Summerfield & Hulton, 1994; Syvitski & Milliman, 2007; Syvitski et al., 2005). When considering the total

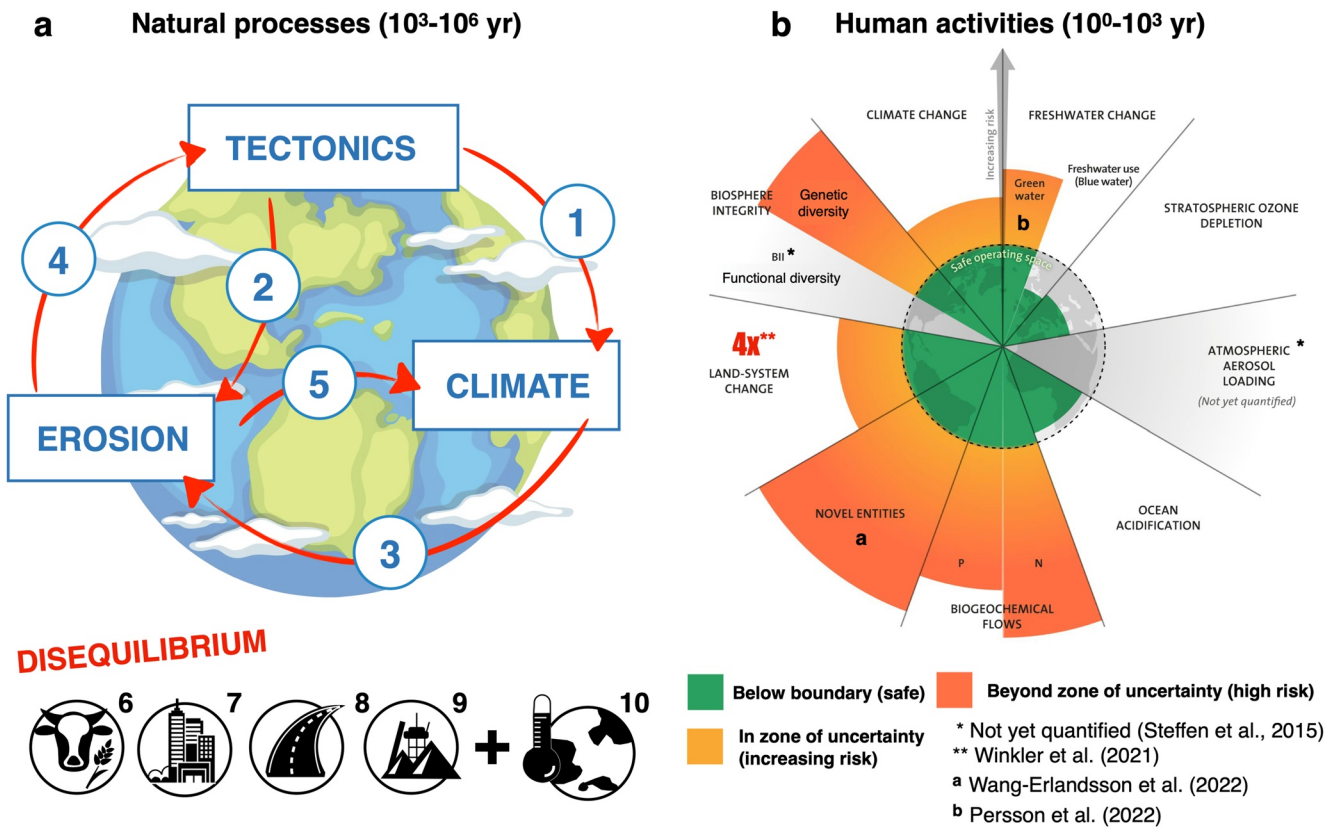


Figure 1. Natural and anthropogenic processes contributing to continental surface evolution over natural and anthropogenic time scales. (a) Feedbacks between tectonics, climate, and erosion. (b) Planetary boundaries (Rockström et al., 2009; Steffen et al., 2015) and status of the control variables (*Azote* for Stockholm Resilience Centre, based on analysis in Wang-Erlandsson et al. (2022)). Keys: (1) orographic barriers and atmospheric circulations; (2) topography, base level changes; (3) vegetation, glaciations; (4) isostasy, exhumation; (5) carbon geological cycle; (6) expansion of croplands and unsustainable practices; (7) urbanization; (8) development of infrastructures; (9) extractive industries; (10) climate change.

ice-free continental surface, this is also equivalent to an average denudation rate of $\approx 60 \text{ mm kyr}^{-1}$ (e.g., Wilkinson & McElroy, 2007).

Bridging these very different time spans, the production of cosmogenic nuclides in the upper few meters of the Earth's surface rocks provides a powerful tool for quantifying denudation rates that integrate the last 10^2 – 10^5 years (Gosse & Phillips, 2001; von Blanckenburg, 2005). In river catchments, this technique is <30-years old, but the global database is growing and covers more and more different climatic and geodynamic contexts (Codilean et al., 2018, 2022; Portenga & Bierman, 2011). For the period 1995–2021, 4,425 measurements of in situ produced ^{10}Be concentrations are included in the Octopus database (Codilean & Munack, 2021), leading to a worldwide median value of about 70 mm kyr^{-1} , and ranging from a few mm kyr^{-1} to a few mm yr^{-1} as in highly dynamic settings like Taiwan (e.g., Derrieux et al., 2014).

In Brazil, in situ produced ^{10}Be -derived rates of denudation only cover a limited part of the territory and are concentrated along the prominent passive margin escarpment of the South Atlantic Ocean and in the Amazon Basin. In the interior of Brazil, a few studies on laterites demonstrated that surface denudation rates can be extremely low (0.2 – 10 mm kyr^{-1}), and largely dependent on lithology (Braucher et al., 1998, 2004; Pupim et al., 2015; Shuster et al., 2012). Recently, Vasconcelos et al. (2019) claimed that such low denudation rates could reveal amongst the oldest landscapes on Earth. Conversely, in Amazonia, catchment-wide, ^{10}Be -derived denudation rates are at least 2 orders of magnitude higher, with values ranging from 200 to 400 mm kyr^{-1} (von Blanckenburg et al., 2012; Wittmann et al., 2012). Along the passive margin escarpment of eastern and southeastern Brazil, basin-wide denudation rates vary significantly as a function of their location with catchments located along the ocean-ward steep topography having rates above 20 mm kyr^{-1} and catchments on the continental plateau having rates below 20 mm kyr^{-1} . The denudation rates also vary according to the eroded lithologies: from

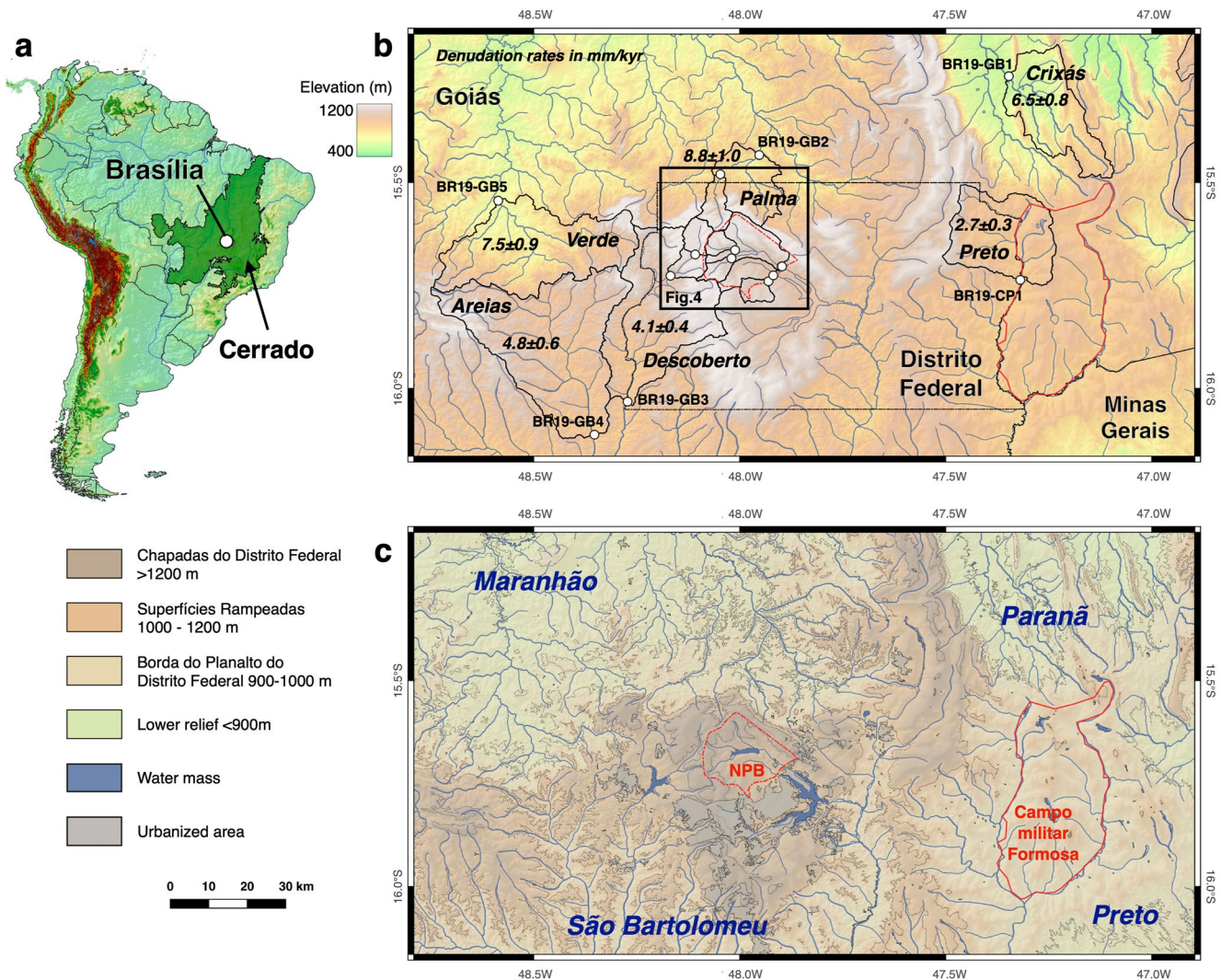


Figure 2. Study area in Central Brazil. (a) Overview map of South America locating Brasília within the Cerrado biome (shown in dark green). (b) Elevation map, extracted from the Space Shuttle Radar Thematic Mapper (SRTM) topographic database at 30-m resolution per pixel (e.g., Reuter et al., 2007), showing the regional distribution of the sampled watersheds (open circles and black polygons). In situ ¹⁰Be-derived denudation values are given in mm kyr⁻¹. See Siame et al. (2023) for supplementary material and analytical results. (c) Geomorphic map showing the regional geomorphic units and drainage networks with main regional watersheds. Red polygons locate the National Park of Brasília (NPB) and the military camp of Formosa, where the Cerrado is preserved.

a few mm kyr⁻¹ in the quartzitic Espinhaço (e.g., Barreto et al., 2013) or the Quadrilátero Ferrífero (e.g., Salgado et al., 2008) to a few tens of mm kyr⁻¹ along the eastern margin escarpment in granite and other igneous rocks (e.g., Cherem et al., 2012; Gonzalez et al., 2016; Salgado et al., 2016; Sordi et al., 2018).

With their rapid and systemic impact on the planet, humans are not merely ordinary geomorphic agents (Hooke, 1994; Turner et al., 1990). Indeed, the Anthropocene refers to a new relationship between humans and the environment in which humanity has become a force that equals or exceeds the natural forcings that shape the Earth system and the biogeochemical cycles or flows that maintain those conditions (e.g., Crutzen, 2002). Even if we can try to go back as far as Paleolithic times to evaluate the amount of ground moved intentionally and unintentionally by humans (e.g., Hooke, 2000), it is considered that the development of agriculture, at the onset of the Bronze Age, as well as growing industrialization and urbanization since the 19th century are responsible for global environmental changes inducing a dramatic increase of continental surface erosion (Ruddiman, 2003, 2007). Based on global RUSLE models, Borrelli et al. (2017) estimated that the worldwide potential soil erosion reached 35–40 Gt in 2012, in agreement with other estimates (Doetterl et al., 2016; Pimentel & Burgess, 2013; Van Oost et al., 2007). They also observed an overall increase of 2.5% during the first decade

of the 21st century, mostly driven by spatial changes of land use, and underlined substantial predicted increases in soil erosion for the less $\approx 3\%$ and least $\approx 12\%$ developed countries. Once distributed over the worldwide surface of croplands ($\approx 1.9 \times 10^9$ ha; e.g., Croplands, 2022), the annual loss estimated by Borrelli et al. (2017) converts into rates of recent surface erosion of about 1,300–1,500 mm kyr⁻¹. This is in line with a global database including >1,500 runoff plots (Xiong et al., 2019), which indicated that anthropogenically disturbed lands such as croplands and orchards are characterized by mean soil losses that are roughly 6 to >100 times the typical values generally measured for undisturbed, natural lands.

To gauge human-induced disturbance on the normal functioning of catchment, cosmogenic nuclides, predominantly in situ produced ¹⁰Be, have long been considered for establishing predisturbance (or natural) denudation rates that can be compared to other proxies such as sediment yields derived from gauging stations (Bartley et al., 2015; E. T. Brown et al., 1998; L. Brown et al., 1998; Hewawasam et al., 2003), geomorphic characteristics and land cover (e.g., Schmidt et al., 2016), or vegetation cover (e.g., Vanacker et al., 2014). Land use impacts on soil erosion were also evaluated in Southern Brazil, using inventories of meteoric ¹⁰Be (Schoonejans et al., 2017) and soil weathering indices (Vanacker et al., 2019) in deeply weathered soils. In Brazil, there is also a large corpus of studies using the universal soil loss equation (see e.g., Gomes et al., 2019; and references in Rosa et al. (2023)) and experimental runoff plots (e.g., Fonseca et al., 2021). According to Borrelli et al. (2021), there are 77 published Brazilian studies dealing with soil erosion, among those 56 provided soil losses by water erosion ranging from 0.1 to 155 t ha⁻¹ yr⁻¹, with a median value of 12.4 t ha⁻¹ yr⁻¹ ($\approx 1,000$ mm kyr⁻¹ with a soil density of about 1,200 kg m⁻³). From an equivalent of 360 plot yr across five Brazilian states, Fonseca et al. (2021) retrieved soil losses ranging from a minimum of 8.9 to a maximum of 205.7 t ha⁻¹ yr⁻¹. They also showed that soil losses under conservation agriculture experience erosion rates that are 70% lower than those measured under conventional agriculture, underlining the importance of permanent vegetation cover to reduce tillage and limit runoff and thus soil erosion (see also Anache et al., 2017, 2019; Castro et al., 1999; Londero et al., 2021).

3. Regional Geomorphic Setting of Brasília

Since several decades, Brazil is a leading agricultural power in the tropics (Hopewell, 2013; Zalles et al., 2019), where the conversion of natural surfaces to produce food and energy is a common land use change, with major expected impacts in the future country's ecosystems (Foley et al., 2005; Margulis et al., 2011) and economy (Rochedo et al., 2018). With 200 million hectares, the Brazilian tropical savanna (Cerrado) is the second most deforested biome in Brazil (Klink & Machado, 2005; Mapbiomas, 2022).

In the 20th century, at the end of the 1930s, the government's policy of national integration favored a slow but steady occupation of the Cerrado that culminated in the early 1960s with the construction of Brasília. This interest is at its peak between the 1960s and 1980s with the development of large government projects like the "Cerrado Occupation and Development Program (PODC)," launched in 1970 for about 15 years, until the early 1980s (Garcia, 1995). The conversion of vast natural vegetation areas into croplands and pastures mainly developed since, following the creation of the capital Brasília and the Federal District. In the last 50 years, the Brazilian Cerrado had 53% of its original vegetation converted into agriculture and pastureland (Beuchle et al., 2015). From 2000 to 2014, Brazilian cropland extent from 26.0 to 46.1 Mha, with 20% from the conversion of natural vegetation, particularly in the Cerrado savanna that was 2.5 times more affected than the Amazon forest (Pennington & Ratter, 2006; Zalles et al., 2019). The Cerrado is thus seriously threatened by the expansion of the agri-food industries, accounting for >60% of Brazilian meat and soybean production, the development of infrastructures, weak legal protections, and rather limited conservation measures (e.g., Strassburg et al., 2017). This large-scale biodiversity and deforestation hotspot is thus an ideal natural laboratory where to analyze the impact of human activities on continental surfaces.

The studied region is located at about 15.5°S and 48.0°W, in the Federal District and stands at the major drainage divides between Maranhão, São Bartolomeu, Preto and Paranã river basins (Figure 2). According to Köppen's climate classification for Brazil (Alvares et al., 2013), the predominant climate in the Federal District is tropical with dry winter (Aw—68%), with local occurrence of humid subtropical with dry winter and hot summer (Cwa—22%), and subtropical with dry winter and temperate summer (Cwb—10%). In Brasília, annual precipitations and temperatures vary from 1,400 to 1,600 mm and from 21° to 22°, respectively (Balbino et al., 2002).

The vegetation of the Cerrado presents a physiognomic gradient determined by edaphic factors such as the depth of the bedrock, the rate and duration of water saturation of the superficial soil horizons, and the rate of base saturation determined by the nature of the bedrock (Balbino et al., 2002; Furley & Ratter, 1988; Oliveira Filho et al., 1989). The Cerrado formations correspond to gallery, dry, and xeromorphic forests with a dominant tree layer (Ribeiro & Walter, 2008). The Cerrado *sensu stricto* is characterized by low, inclined, and tortuous trees (between 3-m and 6-m high), with irregular and twisted branches and evidence of burning (Furley, 1999; Pereira et al., 2014). Shrubs and subshrubs are scattered, with some species characterized by perennial underground organs (xylopods), allowing regrowth after burning or cutting. The trunks of woody plants generally have bark with thick cork, cracked or furrowed, and the apical buds of many species are protected by dense hair. The leaves are stiff and leathery. All these characteristics attest for adaptation to drought conditions. Other Cerrado formations include palm groves on drained soils and “veredas” in hydromorphic areas; herbaceous savannas including *Campo Sujo*, with sparse shrubs and subshrubs, *Campo rupestre*, often associated with rocky, azonal soils, and *Campo limpo*, in which the grass layer is largely predominant. The Cerrado is characterized by a great floristic wealth with >1,000 species of trees and shrubs. Indeed, the densest formations can host up to 150 woody species per hectare (Balbino et al., 2002). For more details about vegetation diversity, one can refer to Righi et al. (2023) who studied above and belowground biomass of Cerrado vegetation encompassing its structural and spatial complexity.

With an area of 424 km², the National Park of Brasília is a protected area, classified under integral protection, which was created shortly after the inauguration of Brasília, in November 1961, to protect the rivers that supply the Federal Capital with drinking water. In this area, the vegetation belongs to the wooded savanna subformation of Cerrado *sensu stricto* (Furley, 1999; Pereira et al., 2014), with a characteristic arboreal cover of 20%–50% and average heights of 3–6 m (Figure 3). It occurs in conjunction with soils showing variable characteristics of color, from light yellow to reddish and dark red, and texture, from sandy to clayey and well-drained (Ribeiro & Walter, 2008). In the Federal District, another area where the Cerrado is well-preserved from deforestation, is the military training camp of Formosa (Figure 2), which, for obvious reasons, was inaccessible for scientific activities.

The central region of Brazil is characterized by a succession of weakly dissected plateaus and strongly dissected areas following a rejuvenation phase, which exposed the Proterozoic metasedimentary and igneous basement rocks. In the Federal District area, three main geomorphic units can be described (Figure 2). With an elevation ranging from 1,200 to 1,300 m, the highest one (*Chapadas do Distrito Federal*) corresponds to flat interfluvial and undulating slopes. It is skirted by reddish and yellowish Ferralsols (World Reference Base for Soil Resources or *Latosolos* in the Brazilian classification; hereafter we used the World Reference Base for Soil Resources and only gave the Brazilian soil terminology equivalent at the first occurrence), with local occurrence of laterites (Reatto et al., 2004), which developed from the Tertiary to Quaternary clay deposits unconformably overlying Neo-Proterozoic metasediments from the Paranoá Group (Moreira et al., 2008). The intermediate unit (*Superfícies Rampeadas*) has elevations between 1,000 and 1,200 m, an average slope of about 10°, and makes an undulating relief connecting the flattened tops to the flat bottoms of the drainage networks (Figure 2). It is characterized by soils varying from yellowish Ferralsols and local laterite occurrences, to Cambisols (*Cambissolos*) with local colluvium occurrences (Reatto et al., 2004). These soils also developed from the Paranoá metasediments (Moreira et al., 2008). The lowest geomorphic unit (*Borda do Planalto do Distrito Federal*) has an elevation comprised between 900 and 1,000 m and corresponds to the headwaters of the regional drainage networks, with rugged relief from northwest to northeast and where Leptosols (*Neossolos liticos*) occur together with local fluvial outcrops (Reatto et al., 2004).

In the Federal District, lands covered by savanna in the National Park coexist with anthropogenically disturbed surfaces that have been cleared and used for agropastoral activities since the creation of the Federal Capital (Figure 3). This part of the plateau is drained by five watersheds within the limits of the park (Torto, Acampamento, Bananal, Barrigudo, and Milho), and two watersheds outside of the park (Rodeador and Palma). Those watersheds are characterized by areas ranging from 34 to 224 km², and relatively low relief characteristics (e.g., Table S1.1 in Siame et al., 2023), except for the Palma River that backwardly eroded the plateau and incised down to the basement rocks. In areas adjacent to the park, such as the Rodeador Watershed (Figure 4), there is a strong consolidation of human activities, with the use of land surfaces for livestock, agriculture, and eucalyptus plantations. In the park, the watersheds drain mostly the highest and intermediate geomorphic units, covered by savanna and Ferralsols, although some may also be affected by human activities along their upstream borders (Figure 4).

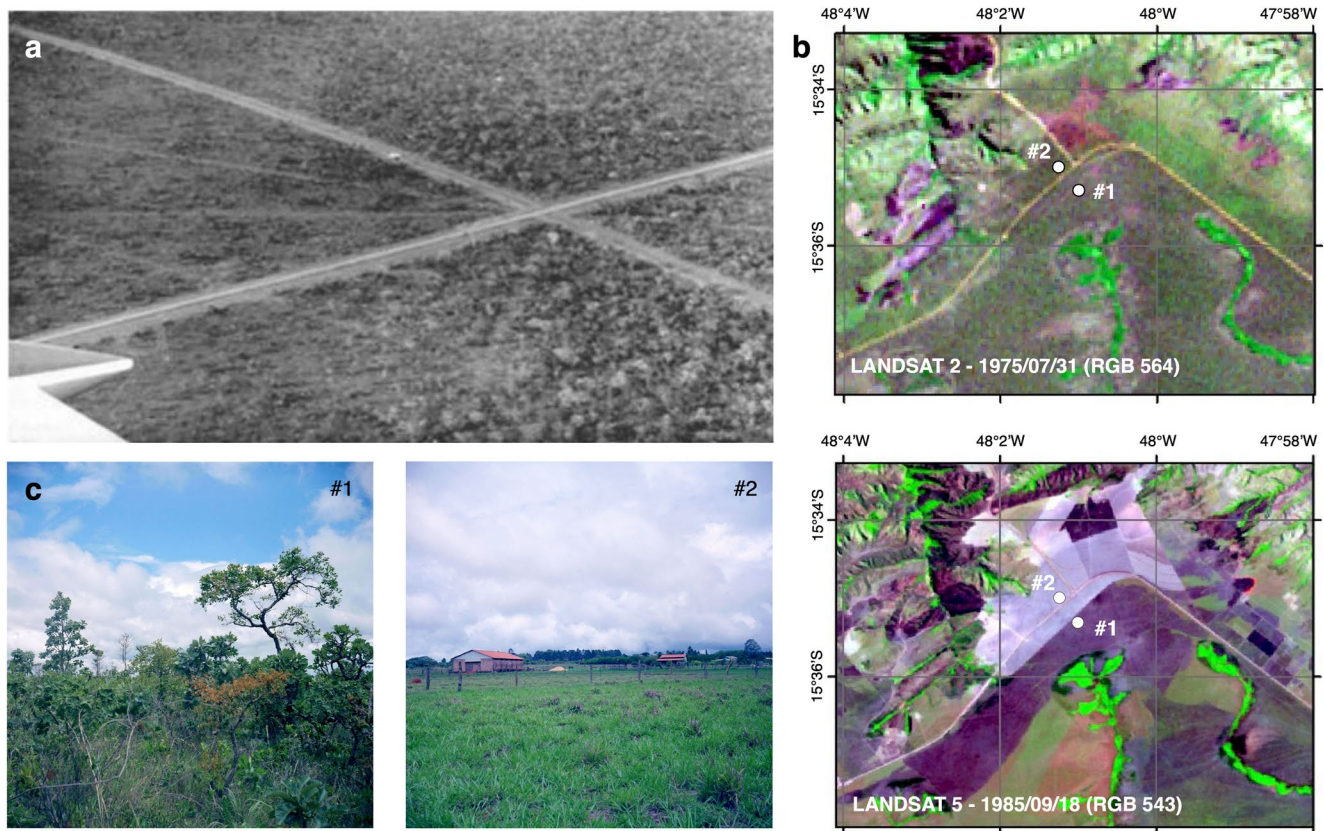


Figure 3. Land use change in the region of Brasília (37 ± 5 years ago). (a) Historical photograph showing the initial crossroad in the Cerrado at the beginning of the construction of Brasília, circa 1958 (Public Archive of the Federal District, Brazil). (b) Extracts of Landsat images showing the change of land use (1975–1985) of surfaces naturally covered by savanna and converted for agropastoral activities at the northern tip of Brasília National Park (Figure 2). Open dots with numbers locate approximately the sites where soil pits were excavated for this study (see Figure 4): #1, pit under Cerrado; #2, pit under agropastoral plot. (c) Field photographs illustrating the landscape inside and outside of the National Park of Brasília at sites of soil pit excavations.

4. Methods

For the long-term trend, in situ and meteoric ^{10}Be cosmogenic nuclide concentrations were used to determine rates of landscape evolution due to natural processes (Figure 5). These include in situ ^{10}Be -derived denudation rates from river-borne sediment (e.g., Granger & Schaller, 2014; von Blanckenburg, 2005), estimates of basin-wide weathering degrees from the measurement of Be-ratio values, that is isotopic ratios between meteoric ^{10}Be and authigenic ^9Be , in the same river-borne sediment (e.g., von Blanckenburg et al., 2012), as well as rates of surface lowering from in situ ^{10}Be in surface boulders (e.g., Lal, 1991) and meteoric $^{10}\text{Be}_m$ inventories in soil profiles (e.g., Graly et al., 2010; Willenbring & von Blanckenburg, 2010). To provide an upper time boundary for the landscape evolution, we also determined the ^{21}Ne concentration in quartz minerals from a ferruginous duricrust outcropping atop of the highest geomorphic surface (Figure 4). For the short-term trend, excess ^{210}Pb and ^{137}Cs activities were measured in the upper 10 cm of the sampled soil profiles (e.g., Arata et al., 2016; He & Walling, 1997). Models of potential soil losses by water erosion (prior to and after land conversion) were elaborated, using the deterministic approach based on the Revised Universal Soil Loss Equation (RUSLE, e.g., Renard et al., 1997, 2011). Graphically summarized in Figure 5, the methods used in this study have long been established in their respective scientific communities. For further information on the technical aspects, analytical findings, and processes involved in determining long-term and recent rates through measuring cosmogenic isotope concentrations and fallout radionuclides activities, as well as RUSLE models, please consult the text file and tables in Siame et al. (2023).

River-borne sediment samples were collected during two fieldwork campaigns in December 2017, at the outlet of watersheds located inside and around the National Park of Brasília (nine samples labeled BR17, Figure 4), and in September 2019, at the outlet of selected catchments from the Maranhão, São Bartolomeu, Preto and Parana

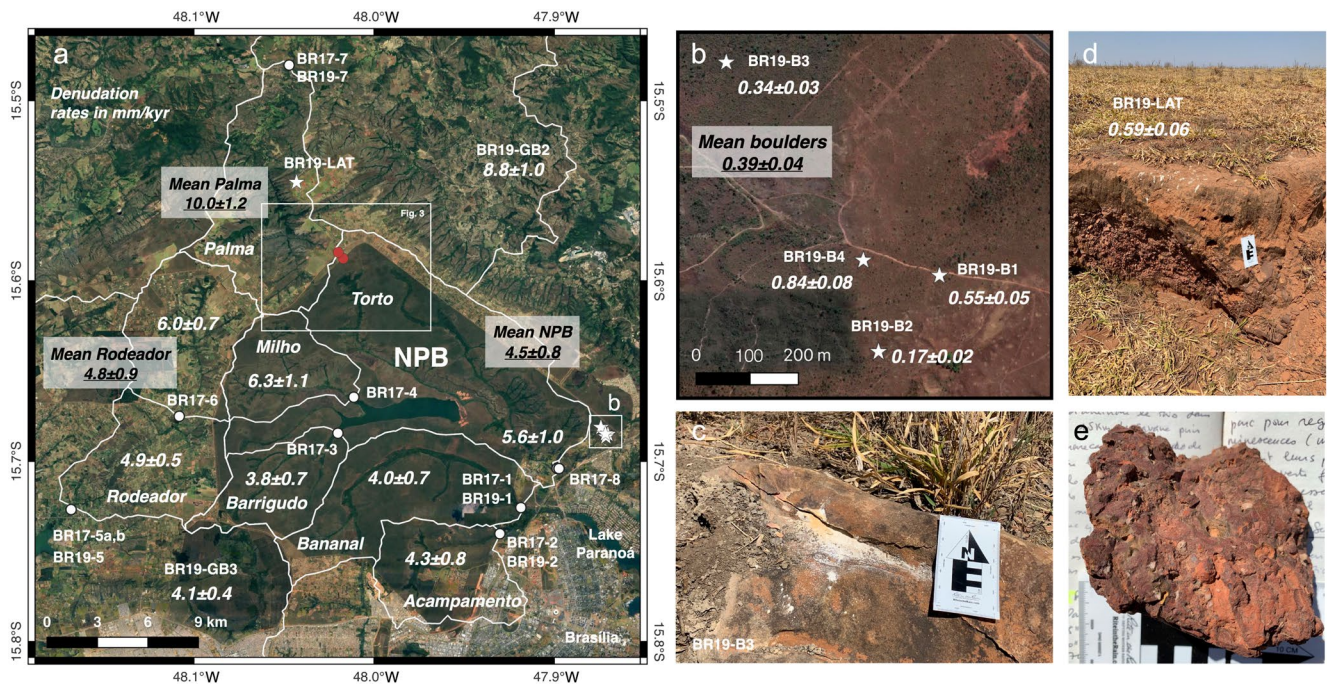


Figure 4. The National Park of Brasília and surroundings. (a) Map locating the sampled watersheds (in situ ^{10}Be and Be-ratio in river-borne sediment; white dots), surface samples (in situ ^{10}Be in quartzite and ^{21}Ne in quartz-bearing duricrust; white stars), as well as the soil pit excavations (meteoric $^{10}\text{Be}_m$, excess ^{210}Pb and ^{137}Cs in Ferralsols; red dots). In situ ^{10}Be -derived denudation values are given in mm kyr^{-1} with uncertainties at $\pm 1\sigma$ (underlined values correspond to mean values calculated from several samples). (b) Enlargement showing the locations of the sampled surface quartzite boulders. (c) Field photograph showing the chiseled top of boulder BR19-B3. (d) Field photograph of the site BR19-LAT showing the lateritic duricrust that partly covers the plateau. (e) Duricrust fragment used to hand-pick quartz minerals for in situ cosmogenic ^{10}Be and ^{21}Ne measurements. Source of the images used for the maps: © CNES/Airbus, Google. See Siame et al. (2023) for supplementary material and analytical results.

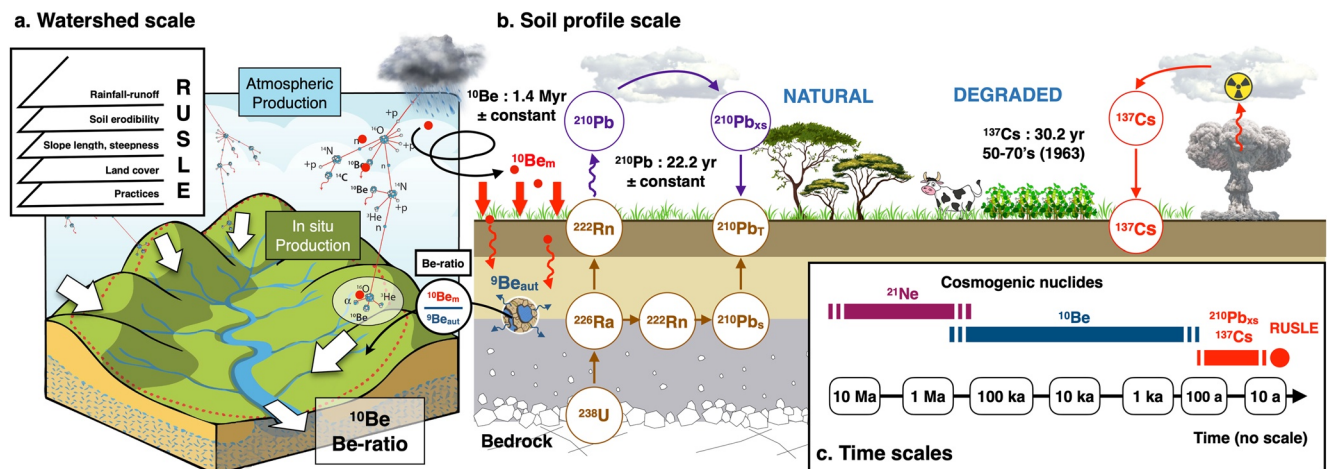


Figure 5. Innovative toolbox tailored to compare natural and degraded land surfaces in Brasília. (a) At the watershed scale: To determine basin-wide denudation rates, we used in situ ^{10}Be concentrations measured in quartz mineral from river-borne sediment (e.g., von Blanckenburg, 2005). In fluvial sediments, the measurement of the Be-ratio (isotopic ratio between meteoric ^{10}Be and authigenic ^9Be) allows determining the degree of chemical weathering at the basin scale (e.g., von Blanckenburg et al., 2012). In surface samples, we measured concentrations of in situ produced ^{10}Be (surface denudation rate) and ^{21}Ne (surface exposure duration). The long time-integrated, basin-wide rates of denudation and chemical erosion can be compared to much shorter time-integrated predictions of soil losses over the same areas by deterministic approaches such as the Revised Universal Soil Loss Equation (RUSLE, e.g., Renard et al., 1997, 2011). (b) At the soil profile scale, $^{10}\text{Be}_m$ inventories allow estimating the long time-integrated rates of surface lowering (e.g., Graly et al., 2010) and soil formation (e.g., Foster et al., 2015). These long-term rates can be compared to recent rates of erosion determined from short-lived, environmental isotopes such as excess ^{210}Pb and ^{137}Cs (e.g., Arata et al., 2016; He & Walling, 1997). (c) Characteristic time scales tackled by the combination of these different approaches.

river systems (eight samples, labeled BR19, Figure 2). During the second fieldwork campaign, replicates for some watersheds inside and outside of the park were also collected to check for possible temporal variability of the cosmogenic signal, as well as four surface samples chiseled atop of quartzite boulders (BR19-B1 to B4, Figure 4) and a sample from a ferruginous duricrust capping the highest geomorphic surface along the edge of the plateau (BR19-LAT, Figure 4). To the East of Brasília, the sampled catchments belong to the Paranã and Preto watersheds and one partly drains the military camp of Formosa (Figure 2). To the East of Brasília, the sampled watersheds belong to the São Bartolomeu and Maranhão rivers. Besides Rio Descoberto, all the watersheds are devoid of heavily urbanized land surfaces (Figure 2). The divides of the selected catchments and the positions of the sampling points are shown in Figures 2 and 4, together with the position of the surface samples. In situ ^{10}Be concentrations were determined in all river-borne and bedrock samples whereas Be-ratio values were determined only for the watersheds sampled around and inside the National Park of Brasília (Figure 4).

For the soil analyses, two $\approx 3\text{-m}$ deep pedological profiles were sampled during the fieldwork campaign of December 2017 in the Ferralsols located inside and outside of the National Park of Brasília (Figure 4). These profiles were excavated by hand down to $\approx 1.7\text{ m}$ and then continued using a hand auger from the floor trench to roughly 3-m depth. The position of the soil pits differs only by the land uses (savanna for pit#1; agropastoral plot for pit#2) whereas they both belong to the same flat topography of the highest geomorphic surface (Figure 4). Soil profiles were continuously sampled down to B-horizon by scraping with metal tools, with a varying depth interval from 2 to 10 cm, between 0-cm and 170-cm depth, and then 20 cm with the hand auger. At selected depths along these profiles, classical pedological and particle-size distribution analyses along with the measurement of meteoric $^{10}\text{Be}_m$ concentrations and short-lived radionuclide activities were performed. All the analytical results are detailed in the Tables S1.2–S1.8 in Siame et al. (2023).

5. Results

5.1. Preanthropogenic Rates Derived From ^{10}Be Cosmogenic Nuclides

5.1.1. Basin-Wide Rates of Denudation

In the State of Goiás and the Federal District, the sampled catchments are characterized by areas ranging from 335 to 1,223 km^2 (Table S1.1, Siame et al., 2023), making them large enough to determine denudation rates that are significant at the regional scale. For these watersheds, in situ ^{10}Be derived denudation rates are ranging from a minimum of 2.7 ± 0.3 to a maximum of $11.1 \pm 1.4\text{ mm kyr}^{-1}$, with median and average values of 6.8 and $7.9 \pm 2.4\text{ mm kyr}^{-1}$, respectively (Figure 6a). The variability in denudation rates observed in regional-scale watersheds can be explained by geomorphic variability. Indeed, denudation rates show a correlation with the mean slope: the steeper the slope, the higher the denudation rates (Figure 6b). While watershed size does not seem to be of primary importance, there is also a trend with local relief: watersheds with greater local relief also exhibit higher denudation rates (Figure 6b). Interestingly, the Palma (BR19-GB2) and Verde (BR19-GB5) rivers exhibit the higher denudation rates and correspond to the headwaters of the Maranhão Watershed that also eroded the Plateau of Brasília through backward erosion (Figures 4 and 6).

In the region around Brasília City (Figure 4), watersheds inside and outside of the park are characterized by in situ ^{10}Be -derived denudation rates ranging from 3.8 ± 0.7 to $6.3 \pm 1.1\text{ mm kyr}^{-1}$, and from 4.6 ± 0.8 to $6.0 \pm 0.8\text{ mm kyr}^{-1}$ (Figure 4 and Table S1.6 in Siame et al., 2023), respectively. In the park, sample BR17-8 was taken at the main outlet, just at the limit of the environmental protection area (Figure 4), yielding a denudation rate of $5.6 \pm 1.0\text{ mm kyr}^{-1}$. The Barrigudo (BR17-3) and Milho (BR17-4) catchments are located upstream of the Torto River (BR17-8), showing in situ ^{10}Be -derived denudation rates of 3.8 ± 0.7 and $6.3 \pm 1.1\text{ mm kyr}^{-1}$, respectively. The Bananal and Acampamento catchments are located upstream of the Lake Paranoá (Figure 4) and drain the southern half of the Park. They were sampled in 2017 and 2019, yielding almost identical in situ ^{10}Be concentrations and thus basin-wide denudation rates of $4.3 \pm 0.8\text{ mm kyr}^{-1}$ (Table S2.2 in Siame et al., 2023). Altogether, the samples taken in the National Park of Brasília yield a mean denudation rate of $4.5 \pm 0.8\text{ mm kyr}^{-1}$ (Table S1.6 in Siame et al., 2023).

Outside of the park, samples were collected along the main drainage of Rodeador and Palma rivers (Figure 4). Along the Rodeador River, samples BR17-6, BR17-5a, and BR19-5 were collected within the riverbed, whereas BR17-5b corresponds to sediment collected on the riverbank. Sample BR19-5 is a replicate of BR17-5a and shows no significant difference of in situ ^{10}Be concentrations. For these three samples, a mean denudation rate of

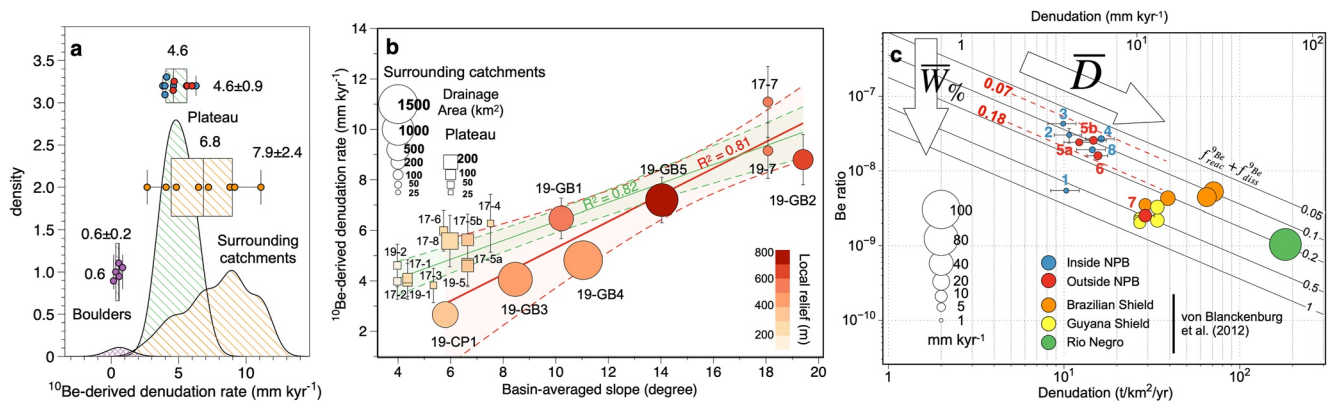


Figure 6. ^{10}Be -derived denudation rates and degree of chemical weathering from river-borne sediments. (a) Probability density functions and whisker boxes for in situ ^{10}Be -derived denudation rates for watershed inside (blue dots) and outside (red dots) the National Park of Brasília (plateau), for surrounding catchments (orange dots) and surface boulders (purple dots). (b) In situ ^{10}Be -derived denudation rates against basin-averaged slopes, with size and colors of the symbols as a function of drainage area (km^2) and local relief (m), respectively. The linear tendencies are given with 95% confidence intervals (dotted lines) for the regional basins only (red) and for combined surrounding catchments and watersheds of the plateau (green). (c) Be-ratio values ($^{10}\text{Be}_m/^{9}\text{Be}_{\text{aut, reac}}$) against in situ ^{10}Be -derived denudation rates (\bar{D} in mm kyr^{-1}) obtained independently from the same samples (see Siame et al., 2023). The contour lines showing a variety of $J^{\text{Be}}_{\text{reac}} + J^{\text{Be}}_{\text{diss}}$ values, expressed in fraction, from 0.1 (almost no chemical weathering, with ^9Be retained in the parent minerals) to 1 (all ^9Be is released by chemical weathering) are calculated with an atmospheric flux of $^{10}\text{Be}_m$ of 0.6×10^6 at. $\text{cm}^{-2} \text{yr}^{-1}$, and a bedrock $[^9\text{Be}]_{\text{parent}}$ of 2.5 mg kg^{-1} (e.g., von Blanckenburg et al., 2012). Bolded red numbers give qualitative estimates of chemical weathering degree ($\bar{W}\%$) for the samples collected inside (blue dots) and outside (red dots) of the National Park of Brasília. Published Be-ratios for Brazilian and Guyana Shield rivers are shown for comparison (von Blanckenburg et al., 2012; Wittmann et al., 2018).

$4.8 \pm 0.9 \text{ mm kyr}^{-1}$ can be calculated, which is in good agreement with the denudation rate of $4.1 \pm 0.4 \text{ mm kyr}^{-1}$ derived from sample BR19-GB3 collected further downstream (Table S1.6 in Siame et al., 2023). Along the Palma River, the sample BR19-7, which is a replicate of BR19-7, exhibits a slightly lower in situ ^{10}Be concentration. Further downstream, and thus averaging a larger part of the Palma River, the sample BR19-GB3 is characterized by a consistent in situ ^{10}Be concentration. For these samples, denudation rates are ranging from 8.8 ± 1.0 to $11.1 \pm 1.2 \text{ mm kyr}^{-1}$, yielding a mean value of $10.0 \pm 1.1 \text{ mm kyr}^{-1}$ (Table S1.6 in Siame et al., 2023).

These results indicate that there is no significant temporal variability of the cosmogenic signal between 2017 and 2019. Altogether, the watersheds on the plateau of Brasília (Plateau group in Figures 6a and 6b) are characterized with median and average values of 4.6 and $4.6 \pm 0.9 \text{ mm kyr}^{-1}$, respectively (Figure 6a). Denudation rates for the anthropogenic (Rodeador) and natural (National Park of Brasília) watersheds are not significantly different. Although exhibiting more variability, the samples taken on the plateau inside and outside the park present the same type of correlation with average slope and size of watersheds (Figure 6b). As previously demonstrated in an agricultural region in Puerto Rico by the pioneering study of E. T. Brown et al. (1998), L. Brown et al. (1998), the cosmogenic signal can remain unaffected by human activities at the watershed scale, provided that these activities are confined to surface-level agricultural practices that do not involve significant excavation and the introduction of sedimentary material with low ^{10}Be concentrations that could inflate denudation rates.

5.1.2. Contribution of Chemical Weathering to Denudation

At the watershed scale, concentrations of in situ produced ^{10}Be are inversely proportional to denudation rate, which corresponds to the sum of mechanical and chemical erosional processes occurring in the source and hillslope areas. To decipher the contribution of these different mechanisms, the isotopic ratio (Be-ratio) between meteoric $^{10}\text{Be}_m$, which continuously accumulates at the surface through humid and dry precipitations (Willenbring & von Blanckenburg, 2010), and the stable, authigenic $^9\text{Be}_{\text{aut}}$, which is released from bedrock at a rate that depends on chemical weathering, can be used (Figure 4). von Blanckenburg et al. (2012) proposed a set of steady state mass balance equations describing this isotopic system, from a soil profile to an entire catchment, as well as the balance between fluids in the regolith and reactive solids formed during chemical weathering. Fluxes of beryllium isotopes, in and out of the weathering zone are in steady state over the time scale of weathering. Thus, assuming that the $^{10}\text{Be}_m$ inventory of the catchment is at steady state (Wittmann et al., 2018), measuring the Be-ratio from the same bulk river-borne fractions than for in situ produced ^{10}Be allows gauging the proportion of chemical weathering that contributes to the total denudation, as measured using in situ ^{10}Be cosmogenic nuclide (von Blanckenburg et al., 2012).

Except for the watershed BR17-1, which is an outlier due to an unexpected high-natural ^9Be content, the Be-ratio measurements are well correlated with in situ ^{10}Be -derived denudation rates and distribute within the array predicted by Equation 9 in von Blanckenburg et al. (2012) (Figure 6c). The watersheds inside and outside the National Park of Brasília are grouped close to the low weathering endmember of the array. Since these watersheds are located atop the plateau and thus only drain areas covered by Ferralsols, this suggests that the denudation of the soils skirting the plateau is dominated by mechanical erosion. Interestingly, sample BR17-7, which corresponds to the Palma Watershed, more incised into the Neo-Proterozoic bedrock, falls within the field of published data for the Brazilian and Guyana cratons close to the Amazon Basin (Figure 6b). These Be-ratio values determined for the watersheds atop the Plateau of Brasília indicate that the regolith that skirts the plateau of Brasília is rather conservative, probably due to an already established heavy depletion resulting from long-lasting exposure, and characterized by basin-wide, chemical weathering rates of about $0.7 \pm 0.3 \text{ mm kyr}^{-1}$, i.e., 7%–18% of the mean values calculated for the watersheds inside and outside of the park (Figure 6b).

5.1.3. Rates of Surface Lowering From In Situ Produced ^{10}Be in Surface Samples

Characterized by Ferralsols and local occurrences of laterites, the surface of the highest geomorphic unit also exhibits isolated and partly embedded boulders of quartzite derived from the Neo-Proterozoic metasediments of the Paranoá Group (Lacerda Filho et al., 2008). At the eastern tip of the National Park of Brasília (Figure 4), samples chiseled atop of such boulders standing roughly 1–2 m above the lateritic surface yielded in situ ^{10}Be -derived denudation rates ranging from 0.2 to 0.9 mm kyr^{-1} (Table S1.6 in Siame et al., 2023), with an average value of $0.6 \pm 0.2 \text{ mm kyr}^{-1}$ (Figure 4). Since these blocks are cut in a resistant quartzite lithology, the denudation rates measured therein are probably representative of the very lower bound surface denudation value for the Plateau of Brasília.

5.1.4. Age Estimate of the Plateau of Brasília From In Situ Produced ^{21}Ne

Along the northern border of the highest geomorphic surface, outcrops of a ferruginous duricrust allowed sampling quartz minerals for in situ produced ^{10}Be and ^{21}Ne (BR19-LAT, Figure 4). The ^{21}Ne concentration is $(203.9 \pm 19.8) \times 10^6 \text{ at. g}^{-1}\text{-SiO}_2$ (Table S1.7 in Siame et al., 2023). In the same quartz minerals, the measured in situ ^{10}Be concentration is $(4.6 \pm 0.1) \times 10^6 \text{ at. g}^{-1}\text{-SiO}_2$ (Table S1.7 in Siame et al., 2023), making the $^{10}\text{Be}/^{21}\text{Ne}$ measured in our sample higher than the production ratio determined by Kober et al. (2011). In the region of Brasília, the quartz derived from Neo-Proterozoic basement rocks (0.5–1.0 Ga) and might thus be contaminated by a significant amount of nucleogenic ^{21}Ne , which could partly explain the observed difference in the production ratio. In our duricrust sample, the quartz grains may have had experienced an initial previous exposure episode several millions of years ago, then followed by a burial episode, before they reached progressively the surface, with a denudation rate of about $0.6 \pm 0.1 \text{ mm kyr}^{-1}$ (e.g., Siame et al., 2023).

Within this framework, the ^{21}Ne concentration most probably represents a minimum cumulated exposure duration, experienced by the quartz grains now embedded in the duricrust, that is between 5.9 ± 0.9 and $13.0 \pm 3.0 \text{ Myr}$ ($9.5 \pm 1.7 \text{ Myr}$) whether (a) using a cosmogenic production scaling scheme accounting for temporal geomagnetic variations or not (e.g., Lifton et al., 2015; Stone, 2000), and (b) correcting for nucleogenic ^{21}Ne content or not (e.g., Siame et al., 2023). This would result amongst the oldest exposure ages determined so far using this cosmogenic nuclide (e.g., Dunai et al., 2005; Schäfer et al., 1999). Altogether, this suggests that the highest geomorphic surface (*Chapada do Distrito Federal*) is most probably polygenic and might result from an etchplanation episode during the Middle-Late Miocene.

5.1.5. Rates of Surface Lowering From Meteoric ^{10}Be Profiles

To estimate a surface lowering rate for the same geomorphic surface, we used $^{10}\text{Be}_m$ inventories in Ferralsols, along the two soil profiles dug under Cerrado forest in the National Park of Brasília and an agropastoral plot close by (Figure 3). Along these profiles, $^{10}\text{Be}_m$ concentrations are of the order of magnitude of $3 \times 10^8 \text{ at. g}^{-1}$ of bulk soil (Table S1.3 in Siame et al., 2023), slightly higher for the profile under the agropastoral plot than for that under Cerrado (Figure 7). Along the first 100 cm, the Cerrado profile shows an almost constant distribution of $^{10}\text{Be}_m$ concentrations with depth, suggesting a long-lasting evolution involving bioturbation and clay translocation that vertically homogenized the concentrations (vertical soil mixing). Conversely, the profile under the agropastoral plot shows a sharp decrease of $^{10}\text{Be}_m$ concentrations in the upper 20 cm of the profile. At depth, both profiles are constant, with slightly higher concentrations along the profile under the agropastoral plot, but both decrease from 150-cm depth (Figure 7).

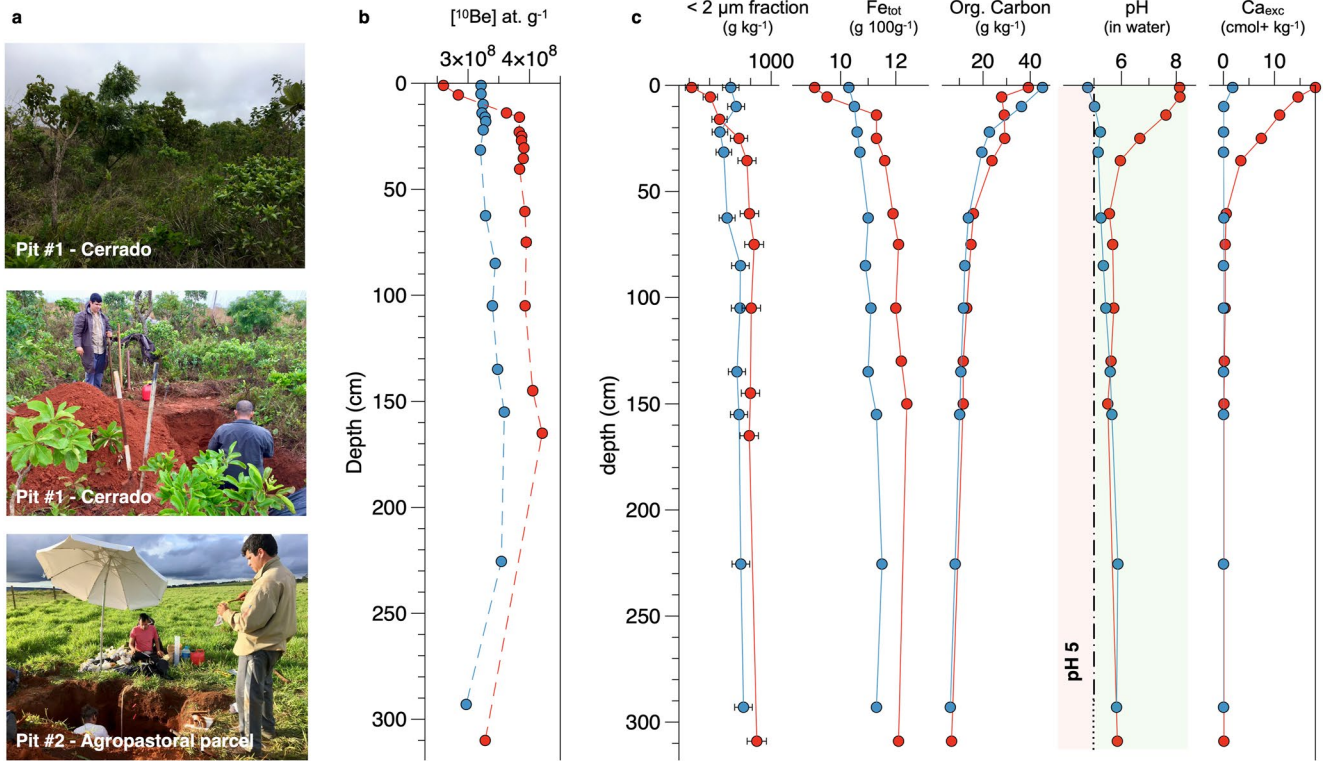


Figure 7. Meteoric $^{10}\text{Be}_m$ concentrations and soil properties along depth profiles in Ferralsols from the highest geomorphic surface. (a) Field photographs showing the excavation sites in the Cerrado (Pit#1) and the agropastoral plot (Pit#2). (b) Meteoric $^{10}\text{Be}_m$ concentrations as a function of depth. (c) Concentrations of $<2\ \mu\text{m}$ fraction, total iron, organic carbon, soil pH in water, and exchangeable calcium and as a function of depth. (d) Clay concentrations against $^{10}\text{Be}_m$ concentrations. Note (1) soil pH in water is higher than 4.5–5.0 except for the first 10 cm under Cerrado, and (2) the depletion of $^{10}\text{Be}_m$ in the first 10 cm of soil under the agropastoral plot consistent with the depletion of $<2\ \mu\text{m}$ fraction concentration in the same layer. See Siame et al. (2023) for supplementary material and analytical results.

Both profiles show a relatively good correlation between $<2\ \mu\text{m}$ fraction, total iron and $^{10}\text{Be}_m$ concentrations (Figure 8), in agreement with what is generally observed since clays, iron oxides, organic matter of this granulometric fraction are prone for beryllium adsorption (e.g., Loba et al., 2022). Conversely, there is no indication along the profiles that $^{10}\text{Be}_m$ are correlated to the soil organic matter content (Figure 8). Along the two profiles, the soil bulk density was measured at selected depths (see Siame et al., 2023). For the Cerrado, it varies from $800\ \text{kg m}^{-3}$ at the soil surface to $1,300\ \text{kg m}^{-3}$ at 1.8-m depth. For the soil under the agropastoral plot, bulk densities are ranging from $1,000$ to $1,100\ \text{kg m}^{-3}$ between 0-m and 1.8-m depth (Table S1.2 in Siame et al., 2023). The bulk densities are thus lower under Cerrado, due to more organic matter and biological activity, than under the agropastoral plot and possibly because of the passage of agriculture machines. In the remainder of the analysis, we will thus consider an average surface density value of 800 and $1,000\ \text{kg m}^{-3}$ for the Ferralsols of the Brazilian Plateau under Cerrado or agricultural activities, respectively.

Along the Cerrado profile, soil pH is ranging from 4.8 to 5.9, slightly increasing with depth. The soil pH along the agropastoral profile strongly varies within the first 50 cm, decreasing from 8.1 to 6.0, and then returns to values comparable to those measured for the Cerrado below 50-cm depth (Figure 7). This strong difference in soil pH is linked to the land use change for agropastoral activities, as also evidenced by the variation of the exchangeable calcium with depth, which is directly linked to soil amending in the upper 50 cm of soil under the agropastoral plot. For organic carbon, the exponential decrease under the Cerrado is typical of natural forest and grassland environments. On the other hand, for the agropastoral plot, the homogeneous concentration between 10-cm and 30-cm depth marks a plowing at 30 cm, with a reincrease of the concentration in the surface horizon due to the installation of the meadow and the abandonment of the plowing.

From the concentrations of $^{10}\text{Be}_m$ and $<2\ \mu\text{m}$ fraction, as well as total iron, organic carbon, pH, and exchangeable calcium, it can thus be underlined that differences of $^{10}\text{Be}_m$ content within the profiles at depth are probably due to lateral variations between the two sampling sites. Additionally, agricultural activities can modify soil

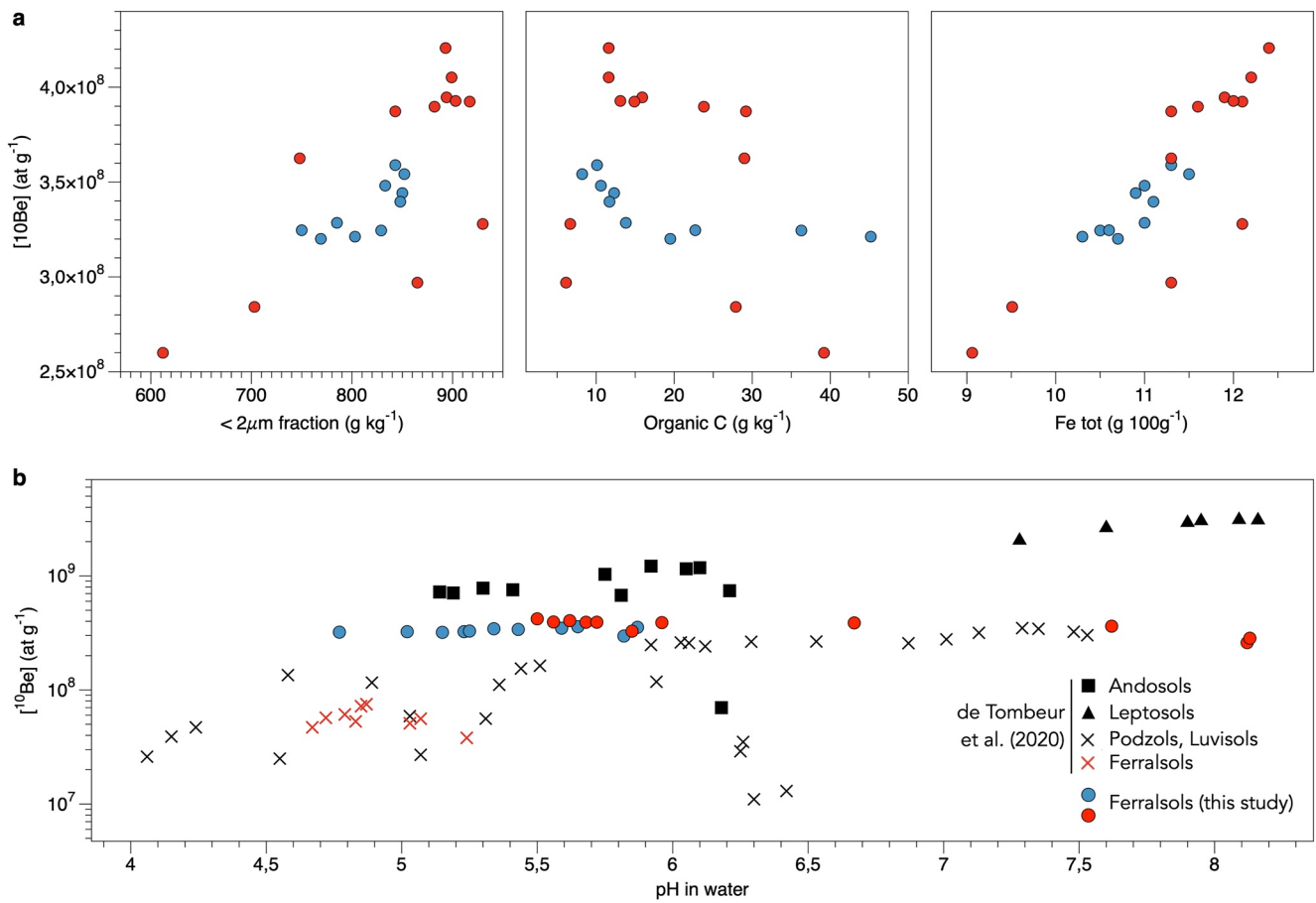


Figure 8. (a) Meteoric $^{10}\text{Be}_m$ concentrations (blue dots, Cerrado; red dots, agropastoral plot) as a function of soil properties ($<2 \mu\text{m}$ fraction concentrations, total iron, organic carbon, soil pH in water) against. (b) Meteoric $^{10}\text{Be}_m$ concentrations as a function of the soil pH (water)—Comparison with other soils (after de Tombeur et al., 2020): an Andosols and a Luvisols under the agropastoral plot, a Ferralsols and a Leptosols under forest and a Podzol both under forest and cultivation. All soils from Europe, except the Ferralsols (French Guyana, under tropical forest).

properties under the agropastoral plot down to 50-cm depth, which impacts different soil processes and changes the soil properties. As a result, the differences in $^{10}\text{Be}_m$ content in the top 20 cm are probably caused by the effects of agriculture on the soil. Conversely, the differences in $^{10}\text{Be}_m$ content observed at depth are more probably due to natural variations between the two profiles, as illustrated by the concentration differences in and $<2 \mu\text{m}$ fraction and iron (Figure 8).

Chemical mobility of $^{10}\text{Be}_m$ has been shown critical for this kind of application (see review by Loba et al., 2022). Indeed, the fixation of $^{10}\text{Be}_m$ in soils depends on pH, soil texture, organic matter (Graly et al., 2010; Pavich et al., 1986; Wyshnytzky et al., 2015; You et al., 1989), as well as the oxyhydroxide content and its enhanced capacity to exchange cations when soil pH in water increases (Vesely et al., 2002). In line with previous studies (Boschi & Willenbring, 2016; Campforts et al., 2016; Takahashi et al., 1999), de Tombeur et al. (2020) found a strong link between meteoric $^{10}\text{Be}_m$ chemical mobility and soil pH in water (Figure 8). In the absence of organic acids, and at pH over 4–5, ^{10}Be generally occurs as hydrolyzed species that are reactive and readily adsorbed onto minerals constituting the $<2 \mu\text{m}$ fraction (de Tombeur et al., 2020; Loba et al., 2022). Although both profiles exhibit pH values that are above or close to this pH threshold for the adsorption of $^{10}\text{Be}_m$ to the soil mineral surfaces, it cannot be totally ruled out that some chemical mobility and thus losses of $^{10}\text{Be}_m$ occurred, as observed by de Tombeur et al. (2020) for Ferralsols under tropical forest in French Guyana (Figure 8).

Inventories (total activities per unit area) were calculated following the method presented in E. T. Brown et al. (1998), L. Brown et al. (1998), and West et al. (2013). Integration at depth used a piecewise cubic Hermite interpolating polynomial (Mathews & Fink, 2004), leading to $^{10}\text{Be}_m$ inventories at 300-cm depth of the order of

magnitude of $(2.8 \pm 0.2) \times 10^{11}$ and $(3.4 \pm 0.3) \times 10^{11}$ at. cm^{-2} for the pits under the Cerrado and the agropastoral plot, respectively (Table S1.3 in Siame et al., 2023). To convert these inventories into surface lowering rates, we assumed that the soils are in steady state, with the rate of meteoric $^{10}\text{Be}_m$ deposition being balanced by the losses due to surface lowering and radioactive decay (e.g., E. T. Brown et al., 1998; L. Brown et al., 1998), ignoring the losses of $^{10}\text{Be}_m$ due to chemical mobility. Using a $^{10}\text{Be}_m$ deposition rate of $(0.5 \pm 0.1) \times 10^6$ at. $\text{cm}^{-2} \text{yr}^{-1}$ for the region of Brasília (Willenbring & von Blanckenburg, 2010), the profiles sampled under Cerrado and the agropastoral plot yield surface lowering rates of 10.7 ± 2.3 and 7.1 ± 1.6 mm kyr^{-1} , respectively, and an averaged value of 8.9 ± 1.9 mm kyr^{-1} (see Siame et al., 2023).

At steady state, if the measured inventories imply equivalent rates of delivery and removal of $^{10}\text{Be}_m$ at the surface of the soil, that is no $^{10}\text{Be}_m$ accumulates because of lateral transport (Schoonejans et al., 2017), minimum regolith residence times of 0.5–1.0 Ma can also be estimated (see Siame et al., 2023). This is not only in agreement with the estimated age of Ferralsols (de Tombeur et al., 2020) but also well supported by the longevity of the plateau surface, as evidenced by cosmogenic exposure dating using ^{21}Ne in the duricrust sample. Finally, at secular equilibrium, if a significant amount of $^{10}\text{Be}_m$ was lost by chemical leaching and deep percolation, the determined inventories should be regarded as minimum values, and the surface lowering rates as maximum values. In southern Brazil and French Guyana, previous studies determined that 50%–70% of the delivered $^{10}\text{Be}_m$ could be leached from such regolith profiles (de Tombeur et al., 2020; Schoonejans et al., 2017). In our case, this would result to an overestimation of surface lowering rates of about 50%–70%, and a 2-fold to 3-fold underestimation of the regolith residence time. Since basin-scale denudation rates determined for the watersheds restricted to the highest geomorphic surface covered by Ferralsols are roughly 5 ± 1 mm kyr^{-1} , this suggests that the amount of $^{10}\text{Be}_m$ lost by chemical mobility in the Ferralsols could well be >50%.

Assuming that the landscape is at steady state implies that both the regolith and the saprolite at depth are only being vertically exhumed by surface lowering. In such a system, the expected total inventory should be the product of the deposition rate with a time scale H/\dot{w} , which corresponds to the time needed to generate a regolith of thickness H at a rate of saprolite-regolith conversion \dot{w} (e.g., Foster et al., 2015). Using Foster et al. (2015)'s formulation of $^{10}\text{Be}_m$ inventories as a function of H and \dot{w} (see Siame et al., 2023), it can be estimated that the regolith should be 10–16-m thick to achieve such a steady state at a rate of about 4–6 mm kyr^{-1} , with an inventory of 6×10^{11} at. cm^{-2} that corresponds to the doubled average value of the estimated inventories to account for $^{10}\text{Be}_m$ chemical mobility. Although speculative, this thickness is not unrealistic for such well-developed soils like the Ferralsols skirting the Plateau of Brasília.

5.2. Anthropogenic Rates of Erosion

5.2.1. Anthropogenic Rates of Erosion Derived From Radionuclide Fallout

Rates of erosion (or deposition) can be quantified using the measurement of fallout radionuclides (e.g., artificial ^{137}Cs and $^{239+240}\text{Pu}$, natural ^{210}Pb , and cosmogenic ^7Be) under different environmental conditions (Mabit et al., 2008; Ritchie & McHenry, 1990; Walling & He, 1997; Zapata, 2002). Like meteoric $^{10}\text{Be}_m$, these radionuclides strongly attach to fine particles at the surface of the soil and follow their movement in the regolith through physical processes. They are thus good tracers of soil and sediment redistribution across the landscape (e.g., Evrard et al., 2016). Their application is based on a comparison of inventories at a given sampling site versus an undisturbed reference site where no erosion nor deposition have occurred.

While various models (profile distribution, inventory, mass balance, diffusion/migration) are available (Lal et al., 2013; Walling & Quine, 1990; Walling et al., 2002), we chose MODERN (Modelling Deposition and Erosion rates with RadioNuclides) because it describes accurately specific depth distributions of any fallout radionuclide at the reference site, and allows adapting it for any specific site conditions (e.g., Arata et al., 2016; and Figure S3.1 in Siame et al., 2023).

The shape of the depth profile for the reference site (Cerrado) is characterized by an excess ^{210}Pb peak in the subsurface horizon with an exponential decline below (Figure 9), with a total inventory of 5,460 Bq m^{-2} (Table S1.8 in Siame et al., 2023). In the agropastoral soil, the sampled profile shows an inventory that is twice lower (2,440 Bq m^{-2}). This difference of inventory results essentially in strong difference of $^{210}\text{Pb}_{xs}$ activities within the first 60 cm of soil and thus to erosion due to land use change during conversion of the land initially covered by the savanna. At both Cerrado and agropastoral sites, the $^{210}\text{Pb}_{xs}$ inventory is measured down to a depth of

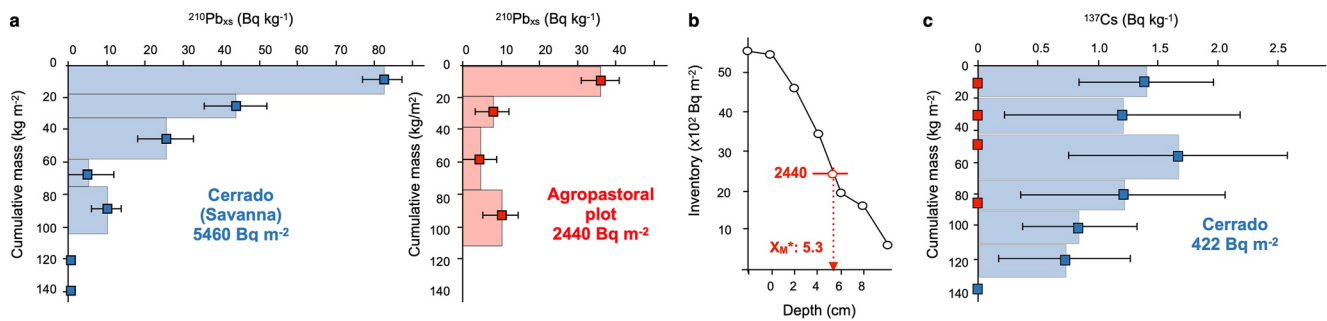


Figure 9. Activities and inventories of fallout radionuclides measured along the first 10 cm of soil excavated in the Cerrado (Pit#1) and the agropastoral (Pit#2) soils. (a) Excess ^{210}Pb activities as a function of depth (expressed as cumulative mass) for Cerrado and agropastoral sampling sites. (b) MODERN results for our case study. The intersect point is 5.3 cm, representing the thickness of soil loss. (c) Activities of ^{137}Cs as a function of depth (expressed as cumulative mass) for Cerrado and agropastoral sample sites.

110 kg m⁻² (roughly 10 cm). Below this cumulative mass of soil, $^{210}\text{Pb}_{\text{ex}}$ activities are below the detection level (Table S1.8 in Siame et al., 2023). By aligning the total inventory of the agropastoral site to the depth profile of the Cerrado site, MODERN returned a soil layer of 5.3 cm affected by soil erosion processes, which corresponds to a rate of $18.0 \pm 2.5 \text{ t ha}^{-1} \text{ yr}^{-1}$ once converted into soil losses for a land use change that occurred 37 ± 5 years ago (Figure 3 and Siame et al., 2023).

The activities of ^{137}Cs measured along the upper 10 cm of soil are low or below detection levels for soil profiles under the Cerrado and the agropastoral plot, respectively (Figure 9). Indeed, the ^{137}Cs activities measured in the Cerrado soil are lower than 1.9 Bq kg^{-1} , as evidenced for areas located around the Equator, between 20°N and 20°S (e.g., Evrard et al., 2020). In the Cerrado soil, the inventory of ^{137}Cs is roughly 422 Bq m^{-2} , which is within the range of values predicted by Chaboche et al. (2021) for this region of Brazil. Since both profiles are only distant by 500 m, we did not interpret the difference in ^{137}Cs activities as a result in a difference of localized precipitations. We rather interpret the absence of ^{137}Cs in the agropastoral soil due to the occurrence of erosion processes at the time of the land use change, which prevented this radionuclide to fix and migrate downward in the soil (e.g., Chaboche et al., 2021). This suggests a soil erosion that is not constant in time, probably faster at the beginning and during the agricultural period, and rather weak since the plot is under pasture because of a higher vegetation cover by grasses.

5.2.2. Anthropogenic Rates of Erosion Derived From RUSLE Models

RUSLE models are erosion prediction approaches (erosion models) that are widely used to predict rates of soil erosion caused by rainfall through surface water erosion (Figure 10), as well as by some linear features, at the level of grooves and furrows (Renard et al., 1997).

As a reference frame, we elaborated an RUSLE prior to human occupation in the region by reclassifying the anthropogenically perturbed areas from the 1970s (Figure S3.3 in Siame et al., 2023), and using morpho-pedological criteria associated with Cerrado classes (soil type and terrain morphology, e.g., Pereira et al., 2014; Ribeiro & Walter, 2008): “typical Cerrado” corresponding to Ferralsols and smooth to gently undulating relief; “forest galleries” corresponding to Gleissols and smooth relief; open woodland or “campo ralo,” corresponding to Neosols and Cambisols for all relief types; and stone woodland or “Cerrado rupestre” for Plintossols with all relief types and Neosols with very steep relief. In this theoretical model, the highest potential soil losses are associated with shrub savanna (*Campo sujo*) and stone woodland (*Cerrado ralo*) classes, with averaged values of about $1 \text{ t ha}^{-1} \text{ yr}^{-1}$ and the lowest to forest galleries, with an averaged value of roughly $0.1 \text{ t ha}^{-1} \text{ yr}^{-1}$ (Table S1.12 in Siame et al., 2023). These natural values of potential soil losses are reflected in the averages calculated for the studied watersheds inside and outside of the National Park, with the Palma River being the catchment with the highest value. Altogether, the RUSLE model for a natural state yields potential soil losses that are significantly lower than $1 \text{ t ha}^{-1} \text{ yr}^{-1}$. In the following, the natural values are subtracted from the potential soil losses modeled for 1975, 1985, and 2018.

For the year 1975, the RUSLE model indicates increased soil losses of $11\text{--}18 \text{ t ha}^{-1} \text{ yr}^{-1}$ and of $0.5\text{--}44.8 \text{ t ha}^{-1} \text{ yr}^{-1}$ inside and outside of the park, respectively (Figure 10). The analysis by watershed indicates that the Milho

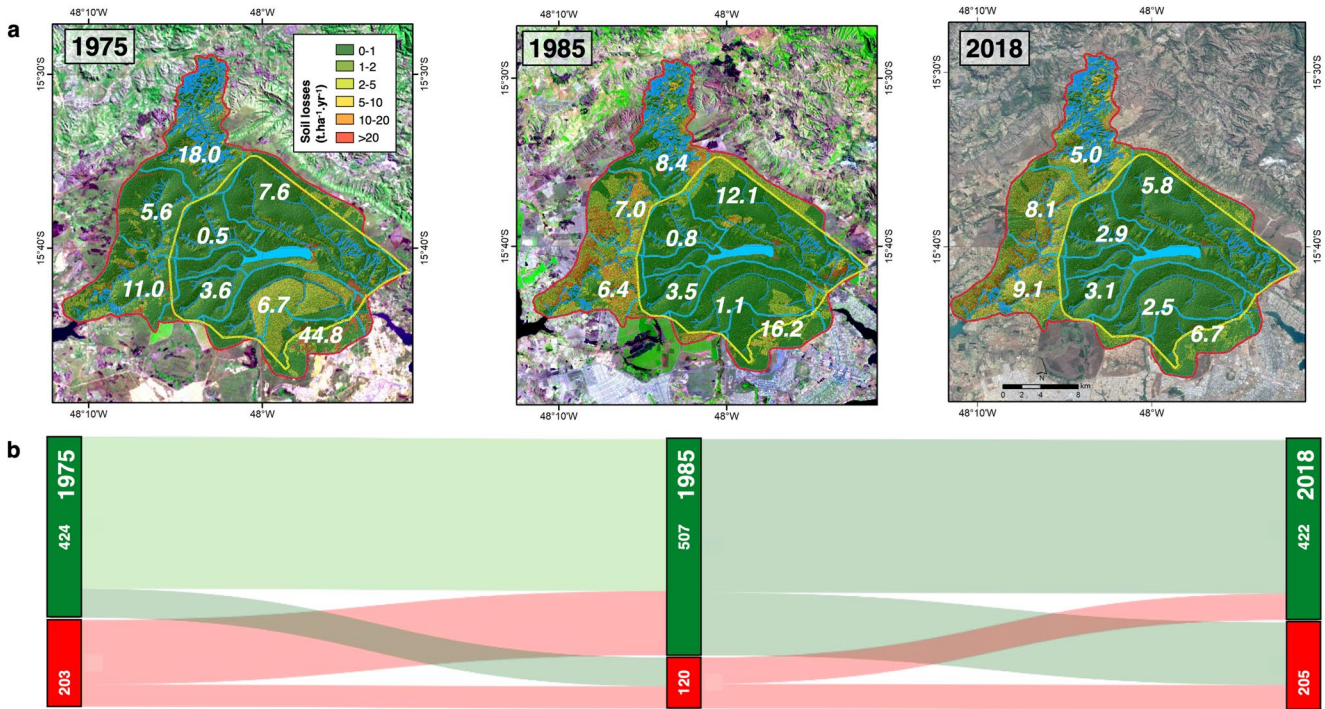


Figure 10. (a) Erosion models for the region around the Park of Brasília, based on the Revised Universal Soil Loss Equation (e.g., Renard et al., 1991, 2011)— $A = R \times K \times LS \times CP$ —where A is the calculated soil loss ($\text{t ha}^{-1} \text{yr}^{-1}$), R is the yearly rainfall runoff erosivity factor ($\text{MJ mm ha}^{-1} \text{h}^{-1}$), K is a soil erodibility factor ($\text{t ha MJ}^{-1} \text{mm}^{-1}$), L is the slope length factor (m), S is the slope steepness factor, C is a cover-management factor, and P is a supporting practice factor. Large italic numbers give the modeled yearly potential soil losses for these watersheds, corrected for the “natural state” elaborated reclassifying the anthropogenically perturbed areas from the 1970s, and using morpho-pedological criteria associated with Cerrado classes. Notes: On the maps, the averaged values are determined using pixel values, but soil losses are mapped using classes. It can thus happen that pixels with very high soil losses occur, due a high K -factor, flux convergence (high LS -factor) or a more exposed soil (high CP -factor), although it is masked by its pixel class. See Siame et al. (2023) for supplementary material information about the RUSLE parameter values. (b) Sankey diagram showing the fluxes of land areas (km^2) between “natural” (green) and “anthropogenic” (red) states during the periods encompassed by the RUSLE models (1975–1985 and 1985–2018). Note that “Anthropogenic” surfaces in 1975 mostly corresponds to burnt surfaces in the southeastern corner of the National Park.

catchment shows the lowest increase of soil losses ($0.8 \text{ t ha}^{-1} \text{yr}^{-1}$), followed by the Bananal Basin ($3.6 \text{ t ha}^{-1} \text{yr}^{-1}$). Together with the Barrigudo Catchment, these watersheds are located at the core of the National Park of Brasília (Figure 4). However, this late basin shows a higher increase of soil losses ($6.7 \text{ t ha}^{-1} \text{yr}^{-1}$) due to a higher contribution of areas with bare soils in 1975. Along the southern edge of the park, the Acampamento Basin is characterized by the greatest soil losses ($44.8 \text{ t ha}^{-1} \text{yr}^{-1}$), followed by the watersheds that are outside of the park. In 1975, the Palma Basin also shows a strong increase of soil losses ($18.0 \text{ t ha}^{-1} \text{yr}^{-1}$), associated mainly with exposed soils due to the creation of local roads and a higher local relief compared to the other watersheds in the area. There is also a strong anthropogenic effect on the Lower Rodeador catchment ($11.0 \text{ t ha}^{-1} \text{yr}^{-1}$), mostly due to a greater contribution of areas with exposed soils due to road cuts and burned areas.

The strong discrepancy between areas inside and outside of the park, which characterizes the RUSLE model for 1975, tends to diminish in 1985. Indeed, during this period, the area of the park suffered from important savanna fires along the northern and southern borders (Figure 10), producing phyto-physiological alterations of the land surfaces. Conversely, the basins located well within the conservation unit showed little variation of potential soil losses when compared to 1975. Interestingly, the increase of yearly soil losses for the Bananal Basin due to forest fire in 1975 appears relatively limited when compared to potential soil losses in 1985 and 2018. This is probably due to the predominantly flat to gently undulating relief with a dominance of Ferralsols, which prevented any accelerated erosion by water runoff after savanna fires in 1975. In 1975 and 1985, anthropogenic activities such as the excavation of surface material for the opening of new roads significantly affected soil losses through water erosion. This is particularly the case for the Acampamento Basin, on the edges of BR-020 road, for the Barrigudo Catchment, along DF-001 road, and along the northern margin of the Torto Watershed (Figure S3.2 in Siame et al., 2023).

Regarding the comparison between the outputs of the 1975 and 1985 RUSLE models, some pixels may show a very high soil loss, due to variables such as soils with high K -factor, flux convergence (high LS -factor), or more exposed soil (high CP -factor). This is especially the case for areas with new settlement areas, whether for grazing, agriculture, or even extraction of materials for civil construction. In these areas, like e.g., the Lower Rodeador Catchment, the mapping of soil losses using classes may mask these high value pixels although they are compatibilized in the average value calculations.

The RUSLE for 2018 appears stabilized for the watersheds located in the park, which are characterized by potential yearly soil losses of about 3–4 and 6–7 t ha⁻¹ yr⁻¹ for the watersheds having their borders affected by human activities. Outside of the park, when compared to the “natural state,” increases of yearly soil losses by water erosion are also ranging between 6 and 10 t ha⁻¹ yr⁻¹. Converting these basin-averaged modeled soil losses into erosion rates, using soil densities of 800 and 1,000 kg m⁻³, yields values ranging from 375 (inside the park) to 1,000 mm kyr⁻¹ (outside the park).

Finally, to address the dynamics of the land cover change during the period of interest (1975–2018), the land use and cover maps were converted into raster images with a spatial resolution of 30 m, allowing for a binary classification of the images into natural (all classes of the Cerrado biome) and anthropogenic (all other types of surface occupation) classes of pixels. From this classification, we derived the Sankey diagram shown in Figure 10 that illustrates the fluxes of land areas passing from natural to anthropogenic states, and vice-versa, between 1975 and 2018.

6. Discussion

6.1. Signification of the ¹⁰Be-Derived Preanthropogenic Rates in Brasília

In this study, basin-wide, ¹⁰Be-derived denudation rates, and surface denudation rates, estimated using river-borne sediment and surface boulders (in situ ¹⁰Be) as well as soil profiles (meteoric ¹⁰Be_m), bracket between 1 and 12 mm kyr⁻¹ and are consistent with the lower bound of published Brazilian denudation rates (see Section 2). However, because of probable ¹⁰Be_m chemical mobility, the rates of surface lowering estimated from ¹⁰Be_m might be overestimated by a factor of 2, which would make them more compatible with the denudation rates determined at the basin scale for the highest geomorphic surface (4.6 ± 0.9 mm kyr⁻¹). In this context, the landscape might be at equilibrium across spatial scales, with rates of basin-wide denudation, soil formation, and surface lowering roughly in balance (Figure 11). An equilibrium that may well be the result of climatic controls on morphogenesis and pedogenesis (e.g., Paisani et al., 2013), with the Ferralsols overlying the Middle-Late Miocene planed surface being most probably rejuvenated during the last 0.5–1.0 Myr.

At a regional scale, the variability of the ¹⁰Be-derived denudation rates is associated with the geomorphic characteristics of the sampled watersheds, such as averaged basin slopes and local relief values (Figure 6a), as it is generally observed in settings of gentle topography (Clementucci et al., 2022, 2023; DiBiase et al., 2010; Ouimet et al., 2009). The rates of geomorphic evolution determined in this study are not surprisingly low and in good agreement with other studies for such relatively low-lying topographic settings (e.g., do Couto et al., 2018; Varajão et al., 2018). The rates of surface lowering derived from ¹⁰Be_m inventories in the current research are also in good agreement with that determined by Schoonejans et al. (2017), though in a much more humid setting of southern Brazil.

There are already a good number of studies that have been interested in comparing denudation rates derived from cosmogenic nuclide concentrations in river sediments with measurements of recent sediment fluxes estimated from solid loads measured at hydrological stations. These studies encompassed different climatic settings and spatial scales (Bartley et al., 2015; E. T. Brown et al., 1998; L. Brown et al., 1998; ; Cox et al., 2009; Gellis et al., 2004; Hewawasam et al., 2003; Kemp et al., 2020; Reusser et al., 2015; Siame et al., 2011; Vanacker et al., 2007, 2014) and calculated recent erosion rates that are significantly higher than long-term cosmogenic-derived denudation rates, owing the discussion of representativeness of short-time versus long-time spans records. They also systematically attributed such an acceleration of erosional processes to land use change of anthropogenic origin. For example, Vanacker et al. (2014) and Bartley et al. (2015) proposed an interesting model where the sensitivity to human-accelerated erosion would be ecosystem dependent, in relation to the potential vegetation cover disturbances because of human impact, producing 100-fold to 1,000-fold increase in erosion compared to natural rates.

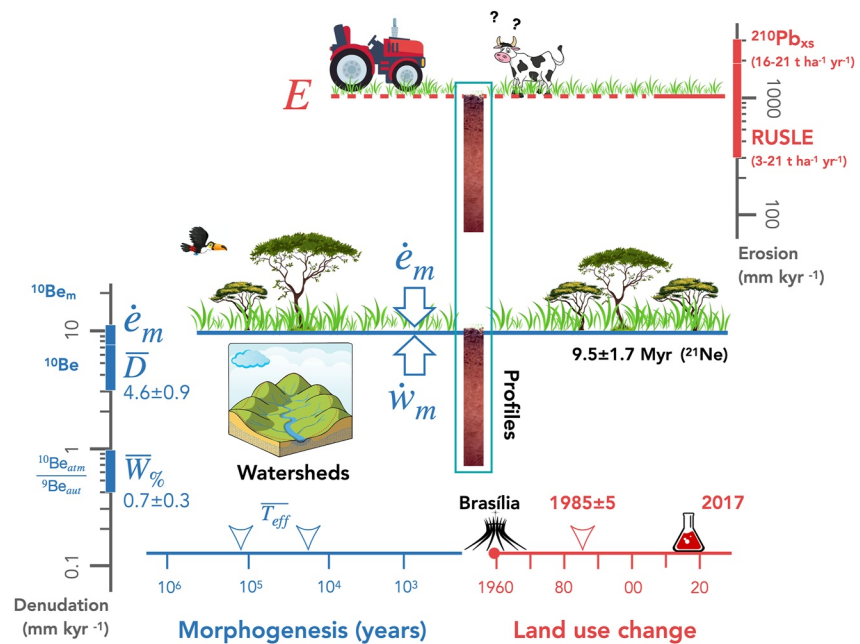


Figure 11. Synthesis of the results obtained in this study. Cosmogenic nuclide concentrations (in situ ^{10}Be) measured in river-borne sediment provide basin-wide denudation rates (\bar{D}) of about a few mm kyr^{-1} , consistent with surface lowering (\dot{e}) and saporlite-regolith conversion rates (\dot{w}) estimated from cosmogenic nuclide concentrations (meteoric ^{10}Be) measured along soil profiles. The proportion of chemical weathering ($\bar{W}_{\%}$), obtained from Be-ratio measurements in river-borne sediment, is roughly 7%–18% of \bar{D} . The age of the plateau is estimated thanks to in situ produced ^{21}Ne cosmogenic exposure dating. The basin-wide denudation rates being almost equal to rates of surface lowering and soil formation, the landscape appears to be in equilibrium across spatial scales. The morphology is long being exposed to in situ production and meteoric deposition, with in situ cosmogenic integration time scales (\bar{T}_{eff}) that are roughly 60–190 kyr (Table S1.6 in Siame et al., 2023). On the short term, land use change is contemporaneous to the development of the Federal District and Brasília City in the late 1950s and early 1960s, which triggered development of agricultural activities and accelerated erosion rates (E) by at least a factor of 160 compared to those of natural processes. Rates are given in mm kyr^{-1} , unless specified.

6.2. Signification of the Recent Erosion Rates in Brasília

From the excess ^{210}Pb mass budget, the rate of soil erosion on the studied grazing land in Brasília region is $\sim 16\text{--}21 \text{ t ha}^{-1} \text{ yr}^{-1}$. This finding aligns well with the values predicted by Borrelli et al. (2017) and the data collected by Xiong et al. (2019) for tropical agriculture and livestock practices. At the scale of the Cerrado Biome, Gomes et al. (2019) also modeled an average value of soil losses by water erosion of about $12 \text{ t ha}^{-1} \text{ yr}^{-1}$, and of about $15 \text{ t ha}^{-1} \text{ yr}^{-1}$ for pastoral plots for the state of Goiás. The RUSLE models determined in the current study for the region of Brasília also predict potential soil losses due to agriculture and livestock that are ranging between 2 and $21 \text{ t ha}^{-1} \text{ yr}^{-1}$ (Table S1.12 in Siame et al., 2023).

Although our investigation is limited to only two soil profiles, it is worth noting that the recent rate of erosion determined for the studied plot using excess ^{210}Pb inventories ($16\text{--}21 \text{ t ha}^{-1} \text{ yr}^{-1}$) fall within the range of the potential soil losses for this type of land use in the same environmental conditions (Table S1.12 in Siame et al., 2023). Without wishing to enter the debate on the representativeness of RUSLE-type soil loss models on large spatial scales, which are difficult to transpose to landscape scales if they are not associated with measurements at the outlet of the watershed, it is finally on plots of this size that they have made it possible to estimate soil erosion rates.

The soil erosion rate determined for the investigated agricultural plot can also be compared with those found for experimental plots in the cultivated Cerrado (Leprun, 1994; Leprun & Brossard, 2000). Balbino et al. (2002) synthesized the data available in the 2000s for soil losses due to water erosion in the Cerrado savanna, including the region of Brasília, and the States of Goiás, Mato Grosso do Sul, and Minas Gerais. The experimental plots were all located on Ferralsols, with a comparable range of annual rainfall, which make them readily comparable to our studied site. For the cultivated plots that were left bare, the soil losses were higher in all cases ($\approx 35 \pm 10 \text{ t ha}^{-1} \text{ yr}^{-1}$). Under soybean ($\approx 6.6 \pm 1.8 \text{ t ha}^{-1} \text{ yr}^{-1}$), and corn ($\approx 15.3 \pm 12.5 \text{ t ha}^{-1} \text{ yr}^{-1}$) crops, losses

were comparable to those commonly observed in Brazil, while under pastures, the observed losses were minimal compared to the previous cases ($0.21 \pm 0.16 \text{ t ha}^{-1} \text{ yr}^{-1}$). On the one hand, such small values might reflect the structure of Ferralsols yielding a higher capacity to infiltrate rainfall under pastures. On the other hand, it should also be noted that these soil erosion data are generally obtained on small plots compared to the cultivated areas typically sampled by the RUSLE method, and only consider water sheet erosion.

In this study, the soil losses of $16\text{--}21 \text{ t ha}^{-1} \text{ yr}^{-1}$ were determined assuming a time window of 37 ± 5 years, to match the major change in land use (1975–1985) with respect to the sampling date (2017). However, as mentioned above, the observation that the ^{137}Cs is totally absent from the soil under the agropastoral plot but measurable in the soil under the Cerrado strongly suggests that the erosion might be essentially linked to the agricultural activities shortly after the change of land use. Under this hypothesis, one possibility would be to consider that all the soil erosion took place during a time frame of 10 years, that is between 1975 and 1985 (Figure 4), yielding yearly soil losses of 65 t ha^{-1} . This maximum value is way above on-site tolerance thresholds of $5\text{--}12 \text{ t ha}^{-1} \text{ yr}^{-1}$ generally accepted for Brazilian soils (Bertoni & Lombardi Neto, 1990; Corrêa et al., 2015), and amongst the highest values of the metaanalysis of runoff plot data provided by Fonseca et al. (2021). Once converted using a soil density of $1,000 \text{ kg m}^{-3}$, the conservative estimate of erosion rate for the agropastoral plot ranges from 1,600 to 2,100 mm kyr^{-1} , which is at least 160 times faster than the natural background values, exceeding by far the sustainability rates of the soil resource estimated from cosmogenic ^{10}Be (Figure 11).

7. Conclusions

This study proposes not only to improve the understanding of natural and anthropogenic soil erosion processes and their interactions but also to better contextualize soil erosion rates in different space and time scales. To this end, we combined various quantification techniques that allows gauging natural and anthropogenic erosion rates at regional and landscape scales, from catchments to soil profiles: in situ produced and meteoric cosmogenic nuclides (^{10}Be), environmental radionuclides (excess ^{210}Pb and ^{137}Cs) as well as water erosion models (RUSLE). Applied to the Cerrado savanna in Central Brazil, this allowed addressing the impact of deforestation and agropastoral activities thanks to a comparison of preanthropogenic denudation and soil formation rates with modern, human-accelerated erosion in the region close to the Federal Capital city of Brasília. This approach shows how intense the land conversion might be to increase surface erosion rates on continental plateaus in the tropics, even in regions that were just recently occupied, like the Brazilian Savanna. This is a promising coupling of methods to foreseeing the impacts of land conversion in the tropical soils of savanna biomes around the globe, as the production of commodities advances at a steady pace.

More specifically, the following conclusions can be drawn from this study:

1. In Central Brazil, the long-term evolution of the landscape is characterized by denudation rates of the order of magnitude of $1\text{--}12 \text{ mm kyr}^{-1}$. This range of values applies to both the denudation rates determined in the catchments (in situ ^{10}Be) and to the lowering of the surface or the conversion of saprolite to regolith (meteoric ^{10}Be). In other words, from a geomorphological point of view, the landscape of the Central Brazilian Plateau in the Brasília region is in equilibrium, probably since the last millions of years as suggested by the pedological characteristics of the studied soil profiles as well as by the long cosmogenic ^{21}Ne surface exposure duration measured in a ferruginous duricrust.
2. In the Brasília region, the change in land use of the surfaces initially covered by the Cerrado savanna is linked to the agro-industrial development and urbanization correlated with the creation of the Federal Capital at the beginning of the 1960s. In our pedological study area, this change of land use occurred between 1975 and 1985, a period during which the savanna was deforested for plowing fields. The annual anthropogenic erosion rates resulting from this change in land use are in the order of $16\text{--}21 \text{ t ha}^{-1} \text{ yr}^{-1}$, when integrated over the last decades, but might be much higher if the erosion took place at the beginning of the agricultural occupation, as suggested by the distribution of fallout radionuclides in the studied soil profiles.

The Anthropocene epoch is appearing just as it becomes imperative to discard the system it describes and to contemplate new political structures and ecological methods. A crucial element of this shift must be an environmental reflexivity built on interdisciplinary exchanges and understanding. While the current study's estimates of soil erosion rates have spatial limitations, we anticipate that it will offer valuable information for shaping effective

conservation policies in the Brazilian Cerrado and contribute to the much-needed environmental awareness arising from the current environmental crisis.

Data Availability Statement

All the necessary information related to the chemical preparations and Accelerator Mass Spectrometry measurements, performed at ASTER-LN2C (Laboratoire National des Nucléides Cosmogéniques, Aix-en-Provence, France), is provided in the Supplementary Material stored in the fair, open science DataSuds of the French National Research Institute for Sustainable Development (see Siame et al., 2023) [Creative Commons Attribution 4.0 International]: <https://doi.org/10.23708/U65XXY>.

References

- Ackermann, O., Greenbaum, N., Bruins, H., Porat, N., Bar-Matthews, M., Almogi-Labin, A., et al. (2014). Palaeoenvironment and anthropogenic activity in the southeastern Mediterranean since the mid-Holocene: The case of Tell es-Safi/Gath, Israel. *Quaternary International*, 328, 226–243. <https://doi.org/10.1016/j.quaint.2014.02.016>
- Alvares, C. A., Stape, J., Sentelhas, P., Gonçalves, J., & Sparoveck, G. (2013). Köppen's climate classification map for Brazil. *Meteorologische Zeitschrift*, 22(6), 711–728. <https://doi.org/10.1127/0941-2948/2013/0507>
- Anache, J. A. A., Wendland, E., Rosalem, L. M. P., Youlton, C., & Oliveira, P. T. S. (2019). Hydrological trade-offs due to different land covers and land uses in the Brazilian Cerrado. *Hydrology and Earth System Sciences*, 23(3), 1263–1279. <https://doi.org/10.5194/hess-23-1263-2019>
- Anache, J. A. A., Wendland, E. C., Oliveira, P. T. S., Flanagan, D. C., & Nearing, M. A. (2017). Runoff and soil erosion plot-scale studies under natural rainfall: A meta-analysis of the Brazilian experience. *Catena*, 152, 29–39. <https://doi.org/10.1016/j.catena.2017.01.003>
- Arata, L., Meusburger, K., Frenkel, E., A'Campo-Neuen, A., Lurian, A. R., Ketterer, M. E., et al. (2016). Modelling Deposition and Erosion rates with RadioNuclides (MODERN)—Part 1: A new conversion model to derive soil redistribution rates from inventories of fallout radionuclides. *Journal of Environmental Radioactivity*, 162, 45–55. <https://doi.org/10.1016/j.jenvrad.2016.05.008>
- Balbino, L. C., Bruand, A., Brossard, M., Grimaldi, M., Hajnos, M., & Guimarães, M. D. F. (2002). Changes in porosity and microaggregation in clayey Ferralsols of the Brazilian Cerrado on clearing for pasture. *European Journal of Soil Science*, 53(2), 219–230. <https://doi.org/10.1046/j.1365-2389.2002.00446.x>
- Barreto, H. N., Varajão, C. A., Braucher, R., Bourlès, D. L., Salgado, A. A., & Varajão, A. F. (2013). Denudation rates of the Southern Espinhaço Range, Minas Gerais, Brazil, determined by in situ-produced cosmogenic beryllium-10. *Geomorphology*, 191, 1–13. <https://doi.org/10.1016/j.geomorph.2013.01.021>
- Bartley, R., Croke, J., Bainbridge, Z. T., Austin, J. M., & Kuhnert, P. M. (2015). Combining contemporary and long-term erosion rates to target erosion hot-spots in the Great Barrier Reef, Australia. *Anthropocene*, 10, 1–12. <https://doi.org/10.1016/j.ancene.2015.08.002>
- Bertoni, J., & Lombardi Neto, F. (1990). *Soil conservation* (3rd ed., p. 355). Icone (in Portuguese).
- Beuchle, R., Grecchi, R. C., Shimabukuro, Y. E., Seliger, R., Eva, H. D., Sano, E., & Achard, F. (2015). Land cover changes in the Brazilian Cerrado and Caatinga biomes from 1990 to 2010 based on a systematic remote sensing sampling approach. *Applied Geography*, 58, 116–127. <https://doi.org/10.1016/j.apgeog.2015.01.017>
- Borrelli, P., Alewell, C., Alvarez, P., Anache, J. A. A., Baartman, J., Ballabio, C., et al. (2021). Soil erosion modelling: A global review and statistical analysis. *Science of the Total Environment*, 780, 146494. <https://doi.org/10.1016/j.scitotenv.2021.146494>
- Borrelli, P., Robinson, D. A., Fleischer, L. R., Lugato, E., Ballabio, C., Alewell, C., et al. (2017). An assessment of the global impact of 21st century land use change on soil erosion. *Nature Communications*, 8(1), 2013. <https://doi.org/10.1038/s41467-017-02142-7>
- Boschi, V., & Willenbring, J. (2016). The effect of pH, organic ligand chemistry and mineralogy on the sorption of beryllium over time. *Environmental Chemistry*, 13(4), 711–722. <https://doi.org/10.1071/en15107>
- Brantley, S. L., Goldhaber, M. B., & Ragnarsdottir, K. V. (2007). Crossing disciplines and scales to understand the critical zone. *Elements*, 3(5), 307–314. <https://doi.org/10.2113/gselements.3.5.307>
- Braucher, R., Bourlès, D. L., Colin, F., Brown, E. T., & Boulange, B. (1998). Brazilian laterite dynamics using in situ-produced ¹⁰Be. *Earth and Planetary Science Letters*, 163(1–4), 197–205. [https://doi.org/10.1016/s0012-821x\(98\)00187-3](https://doi.org/10.1016/s0012-821x(98)00187-3)
- Braucher, R., Lima, C. V., Bourlès, D. L., Gaspar, J. C., & Assad, M. L. L. (2004). Stone-line formation processes documented by in situ-produced ¹⁰Be distribution, Jardim River basin, DF, Brazil. *Earth and Planetary Science Letters*, 222(2), 645–651. <https://doi.org/10.1016/j.epsl.2004.02.033>
- Brown, E. T., Stallard, R. F., Larsen, M. C., Bourlès, D. L., Raisbeck, G. M., & Yiu, F. (1998). Determination of predevelopment denudation rates of an agricultural watershed (Cayaguas River, Puerto Rico) using in-situ-produced ¹⁰Be in river-borne quartz. *Earth and Planetary Science Letters*, 160(3–4), 723–728. [https://doi.org/10.1016/s0012-821x\(98\)00123-x](https://doi.org/10.1016/s0012-821x(98)00123-x)
- Brown, L., Pavich, M. J., Hickman, R. E., Klein, J., & Middleton, R. (1988). Erosion of the eastern United States observed with ¹⁰Be. *Earth Surfaces, Processes and Landforms*, 13(5), 441–457. <https://doi.org/10.1002/esp.3290130509>
- Campforts, B., Vanacker, V., Vanderborght, J., Baken, S., Smolders, E., & Govers, G. (2016). Simulating the mobility of meteoric ¹⁰Be in the landscape through a coupled soil-hillslope model (Be2D). *Earth and Planetary Science Letters*, 439, 143–157. <https://doi.org/10.1016/j.epsl.2016.01.017>
- Castro, N. M. R., Auzet, A. V., Chevallier, P., & Leprun, J. C. (1999). Land use change effects on runoff and erosion from plot to catchment scale on the basaltic plateau of southern Brazil. *Hydrological Procedure*, 13(11), 1621–1628. [https://doi.org/10.1002/\(sici\)1099-1085\(19990815\)13:11<1621::aid-hyp831>3.0.co;2-1](https://doi.org/10.1002/(sici)1099-1085(19990815)13:11<1621::aid-hyp831>3.0.co;2-1)
- Chaboche, P.-A., Saby, N. P. A., Lacey, J. P., Minella, J. P. G., Tiecher, T., Ramon, R., et al. (2021). Mapping the spatial distribution of global ¹³⁷Cs fallout in soils of South America as a baseline for Earth Science studies. *Earth-Science Reviews*, 214, 103542. <https://doi.org/10.1016/j.earscirev.2021.103542>
- Cherem, L. F. S., Varajão, C. A. C., Braucher, R., Bourlès, D., Salgado, A. A. R., & Varajão, A. C. (2012). Long-term evolution of denudational escarpments in southeastern Brazil. *Geomorphology*, 173, 118–127. <https://doi.org/10.1016/j.geomorph.2012.06.002>

Acknowledgments

The authors would like to thank the Franco-Brazilian framework for scientific collaboration (CAPES-COFECUB) for its continuous support (projects 869/15 and 981/20) as well as the EC2CO Structuring Initiative (Hybige) of the Institut National des Sciences de l'Univers (INSU, CNRS, France) for its financial participation to the chemical analyses. This study also received financial supports from the CEREGE laboratory (APIC Research project). The ASTER AMS national facility (CEREGE, Aix-en-Provence) is supported by INSU/CNRS, the ANR through the Projets thématiques d'excellence programme for the Equipements d'Excellence (ASTER-CEREGE action), the IRD, and the University of Aix-Marseille. Lionel Siame is grateful to IRD for the continuing support through the "Mission de Longue Durée" mobility program. The authors warmly thank Veerle Vanacker and Michel Brossard, as well as an anonymous reviewer, for their thorough reading and very helpful comments on a draft of the manuscript. We also thank the editorial team of Earth's Future for the efficient management of our manuscript during the review and editing process. The authors declare no conflicts of interest relevant to this study.

- Clementucci, R., Ballato, P., Siame, L., Faccenna, C., Yaaqoub, A., Essaifi, A., et al. (2022). Lithological control on erosional dynamics in a tectonically inactive mountain belt (Anti-Atlas, Morocco). *Earth and Planetary Science Letters*, 596, 117788. <https://doi.org/10.1016/j.epsl.2022.117788>
- Clementucci, R., Ballato, P., Siame, L., Fox, M., Lanari, R., Sembroni, A., et al. (2023). Surface uplift and topographic rejuvenation of a tectonically inactive range: Insights from the Anti-Atlas and the Siroua Massif (Morocco). *Tectonics*, 42, e2022TC007383. <https://doi.org/10.1029/2022TC007383>
- Codilean, A. T., & Munack, H. (2021). OCTOPUS Database v.2: The CRN Denudation Global collection. Basin-averaged denudation rates from cosmogenic Be-10 and Al-26 abundances (1995–2021). <https://doi.org/10.25900/g76f-0h4>
- Codilean, A. T., Munack, H., Cohen, T. J., Saktura, W., Gray, A. G., & Mudd, S. M. (2018). Octopus: An open cosmogenic isotope and luminescence database. *Earth System Science Data Discussions*, 10(4), 2123–2139. <https://doi.org/10.5194/essd-10-2123-2018>
- Codilean, A. T., Munack, H., Saktura, W. M., Cohen, T. J., Jacobs, Z., Ulm, S., et al. (2022). OCTOPUS Database v. 2. *Earth System Science Data Discussions*, 14(8), 3695–3713. <https://doi.org/10.5194/essd-14-3695-2022>
- Corrêa, E., Moraes, I., & Pinto, S. (2015). Estimating soil erodibility and soil loss tolerance of the mideastern São Paulo state. *Geociencias*, 34, 848–860.
- Covault, J. A., Craddock, W. H., Romans, B. W., Fildani, A., & Gosai, M. (2013). Spatial and temporal variations in landscape evolution: Historic and longer-term sediment flux through global catchments. *The Journal of Geology*, 121(1), 35–36. <https://doi.org/10.1086/668680>
- Cox, R., Bierman, P., Jungers, M. C., & Rakotondrazafy, A. F. M. (2009). Erosion rates and sediment sources in Madagascar inferred from ¹⁰Be analysis of Lavaka, slope, and river sediment. *The Journal of Geology*, 117(4), 363–376. <https://doi.org/10.1086/598945>
- Croplands. (2022). Retrieved from <https://www.usgs.gov/media/images/cropland-percent-total-global-cropland>
- Cruzten, P. J. (2002). Geology of mankind. *Nature*, 415(6867), 23. <https://doi.org/10.1038/415023a>
- Derrière, F., Siame, L. L., Bourlès, D. L., Chen, R. F., Braucher, R., Léanni, L., et al. (2014). How fast is the denudation of the Taiwan mountain belt? Perspectives from in situ cosmogenic ¹⁰Be. *Journal of Asian Earth Sciences*, 88, 230–245. <https://doi.org/10.1016/j.jseaes.2014.03.012>
- de Tombeur, F., Cornu, S., Bourlès, D., Duvivier, A., Pupier, J., Team ASTER, et al. (2020). Retention of ¹⁰Be, ¹³⁷Cs and ²¹⁰Pbxs in soils: Impact of physico-chemical characteristics. *Geoderma*, 367, 114242. <https://doi.org/10.1016/j.geoderma.2020.114242>
- DiBiase, R. A., Whipple, K. X., Heimsath, A. M., & Ouimet, W. B. (2010). Landscape form and millennial erosion rates in the San Gabriel Mountains, CA. *Earth and Planetary Science Letters*, 289(1–2), 134–144. <https://doi.org/10.1016/j.epsl.2009.10.036>
- Dirzo, R., Young, H. S., Galetti, M., Ceballos, G., Isaac, N. J. B., & Collen, B. (2014). Defaunation in the Anthropocene. *Science*, 345(6195), 401–406. <https://doi.org/10.1126/science.1251817>
- do Couto, E. V., dos Santos, L. J. C., de Sordi, M. V., Bourlès, D., Braucher, R., Salgado, A. A. R., et al. (2018). Changes of the base levels in the Ivai and Paraná Rivers confluence zone (Southern Brazil): Denudational reflexes in the evolution of the upstream drainage network. *Zeitschrift für Geomorphologie*, 62(1), 23–40. <https://doi.org/10.1127/zfg/2018/0545>
- Doetterl, S., Berhe, A. A., Nadeu, E., Wang, Z., Sommer, M., & Fiener, P. (2016). Erosion, deposition, and soil carbon: A review of process-level controls, experimental tools, and models to address C cycling in dynamic landscapes. *Earth-Science Reviews*, 154, 102–122. <https://doi.org/10.1016/j.earscirev.2015.12.005>
- Dunai, T. J., López, G. A. G., & Juez-Larré, J. (2005). Oligocene-Miocene age of aridity in the Atacama Desert revealed by exposure dating of erosion-sensitive landforms. *Geology*, 33(4), 321–324. <https://doi.org/10.1130/g21184.1>
- Ellis, E. C., Gauthier, N., Klein Goldewijk, K., Bliege Bird, R., Boivin, N., Díaz, S., et al. (2021). People have shaped most of terrestrial nature for at least 12,000 years. *Proceedings of the National Academy of Sciences of the United States of America*, 118(17), e2023483118. <https://doi.org/10.1073/pnas.2023483118>
- Euzen, A., Lavelle, B., & Thiebault, S. (2017). *L'adaptation au changement climatique—Une question de sociétés*. CNRS Editions.
- Evrard, O., Chaboche, P. A., Ramon, R., Foucher, A., & Lacey, J. P. (2020). A global review of sediment source fingerprinting research incorporating fallout radiocesium (¹³⁷Cs). *Geomorphology*, 362, 107103. <https://doi.org/10.1016/j.geomorph.2020.107103>
- Evrard, O., Lacey, J. P., Huon, S., Lefèvre, I., Sengtaheuanghoung, O., & Ribolzi, O. (2016). Combining multiple fallout radionuclides (¹³⁷Cs, ⁷Be, ²¹⁰Pbxs) to investigate temporal sediment source dynamics in tropical, ephemeral riverine systems. *Journal of Soils and Sediments*, 16(3), 1130–1144. <https://doi.org/10.1007/s11368-015-1316-y>
- Ferdinand, M. (2019). *Une Écologie Décoloniale. Penser L'écologie Depuis Le Monde Caribéen*. Seuil.
- Foley, J. A., DeFries, R., Asner, G. P., Barford, C., Bonan, G., Carpenter, S. R., et al. (2005). Global consequences of land use. *Science*, 309(5734), 570–574. <https://doi.org/10.1126/science.1111772>
- Fonseca, M. R. S., Uagoda, R., & Chaves, H. M. L. (2021). Rates, factors, and tolerances of water erosion in the Cerrado biome (Brazil): A meta-analysis of runoff plot data. *Earth Surface Processes and Landforms*, 47(2), 582–595. <https://doi.org/10.1002/esp.5273>
- Foster, M. A., Anderson, R. S., Wyshnytzky, C. E., Ouimet, W. B., & Dethier, D. P. (2015). Hillslope lowering rates and mobile-regolith residence times from in situ and meteoric ¹⁰Be analysis, boulder creek critical zone observatory, Colorado. *Geological Society of America Bulletin*, 127(5–6), 862–878. <https://doi.org/10.1130/b31115.1>
- Furley, P. A. (1999). The nature and diversity of neotropical savanna vegetation with particular reference to the Brazilian Cerrados. *Global Ecology and Biogeography*, 8(3–4), 223–241. <https://doi.org/10.1046/j.1365-2699.1999.00142.x>
- Furley, P. A., & Ratter, J. A. (1988). Soil resources and plant communities of the central Brazilian Cerrado and their development. *Journal of Biogeography*, 15(1), 97–108. <https://doi.org/10.2307/2845050>
- Garcia, E. A. C. (1995). Desenvolvimento econômico sustentável do Cerrado. *Pesquisa Agropecuária Brasileira*, 30(6), 759–774.
- Gellis, A. C., Pavich, M. J., Bierman, P. R., Clapp, E. M., Ellevein, A., & Aby, S. (2004). Modern sediment yield compared to geologic rates of sediment production in a semi-arid basin, New Mexico: Assessing the human impact. *Earth Surface Processes and Landforms: The Journal of the British Geomorphological Research Group*, 29(11), 1359–1372. <https://doi.org/10.1002/esp.1098>
- Gomes, L., Simões, S. J., Dalla Nora, E. L., de Sousa-Neto, E. R., Forti, M. C., & Ometto, J. P. H. (2019). Agricultural expansion in the Brazilian Cerrado: Increased soil and nutrient losses and decreased agricultural productivity. *Land*, 8(1), 12. <https://doi.org/10.3390/land8010012>
- Gonzalez, V. S., Bierman, P. R., Fernandes, N. F., & Rood, D. H. (2016). Long-term background denudation rates of southern and southeastern Brazilian watersheds estimated with cosmogenic ¹⁰Be. *Geomorphology*, 268, 54–63. <https://doi.org/10.1016/j.geomorph.2016.05.024>
- Gosse, J. C., & Phillips, F. M. (2001). Terrestrial in situ cosmogenic nuclides: Theory and application. *Quaternary Science Reviews*, 20(14), 1475–1560. [https://doi.org/10.1016/s0277-3791\(00\)00171-2](https://doi.org/10.1016/s0277-3791(00)00171-2)
- Graly, J. A., Bierman, P. R., Reusser, L. J., & Pavich, M. J. (2010). Meteoric ¹⁰Be in soil profiles—A global meta-analysis. *Geochimica et Cosmochimica Acta*, 74(23), 6814–6829. <https://doi.org/10.1016/j.gca.2010.08.036>
- Granger, D. E., & Schaller, M. (2014). Cosmogenic nuclides and erosion at the watershed scale. *Elements*, 10(5), 369–373. <https://doi.org/10.2113/gselements.10.5.369>

- He, Q., & Walling, D. E. (1997). The distribution of fallout ^{137}Cs and ^{210}Pb in undisturbed and cultivated soils. *Applied Radiation and Isotopes*, 48(5), 677–690. [https://doi.org/10.1016/s0969-8043\(96\)00302-8](https://doi.org/10.1016/s0969-8043(96)00302-8)
- Herman, F., & Champagnac, J.-D. (2016). Plio-Pleistocene increase of erosion rates in mountain belts in response to climate change. *Terra Nova*, 28(1), 2–10. <https://doi.org/10.1111/ter.12186>
- Hewawasam, T., von Blanckenburg, F., Schaller, M., & Kubik, P. (2003). Increase of human over natural erosion rates in tropical highlands constrained by cosmogenic nuclides. *Geology*, 31(7), 597–600. [https://doi.org/10.1130/0091-7613\(2003\)031<0597:iophone>2.0.co;2](https://doi.org/10.1130/0091-7613(2003)031<0597:iophone>2.0.co;2)
- Hooke, R. L. (1994). On the efficacy of humans as geomorphic agents. *Geological Society of America Today*, 4(9), 217.
- Hooke, R. L. (2000). On the history of humans as geomorphic agents. *Geology*, 28(9), 843–846. [https://doi.org/10.1130/0091-7613\(2000\)028<0843:othoha>2.3.co;2](https://doi.org/10.1130/0091-7613(2000)028<0843:othoha>2.3.co;2)
- Hopewell, K. (2013). New protagonists in global economic governance: Brazilian agribusiness at the WTO. *New Political Economy*, 18(4), 603–623. <https://doi.org/10.1080/13563467.2013.736957>
- IPCC. (2019). Climate change and land: An IPCC special report on climate change, desertification, land degradation, sustainable land management, food security, and greenhouse gas fluxes in terrestrial ecosystems. In P. R. Shukla, J. Skea, E. Calvo Buendia, V. Masson-Delmotte, H.-O. Pörtner, D. C. Roberts, et al., (Eds.), *Intergovernmental Panel on Climate Change* (p. 864).
- Kemp, D. B., Sadler, P. M., & Vanacker, V. (2020). The human impact on North American erosion, sediment transfer, and storage in a geologic context. *Nature Communications*, 11(1), 6012. <https://doi.org/10.1038/s41467-020-19744-3>
- Klink, C. A., & Machado, R. B. (2005). Conservation of the Brazilian Cerrado. *Conservation Biology*, 19(3), 707–713. <https://doi.org/10.1111/j.1523-1739.2005.00702.x>
- Kober, F., Alfimov, V., Ivy-Ochs, S., Kubik, P. W., & Wieler, R. (2011). The cosmogenic ^{21}Ne production rate in quartz evaluated on a large set of existing ^{21}Ne - ^{10}Be data. *Earth and Planetary Science Letters*, 302(1–2), 163–171. <https://doi.org/10.1016/j.epsl.2010.12.008>
- Kummu, M., Heino, M., Taka, M., Varis, O., & Viviroli, D. (2021). Climate change risks pushing one-third of global food production outside the safe climatic space. *One Earth*, 4(4), 720–729. <https://doi.org/10.1016/j.oneear.2021.04.017>
- Lacerda Filho, J. V., Moreira, M. L. O., Moreton, L. C., Araújo, V. A., & Costa, H. F. C. (2008). Geologia do Estado de Goiás e Distrito Federal. Escala 1: 500.000. *Goiânia: CPRM/SIC—FUNMINERAL*.
- Lal, D. (1991). Cosmic ray labeling of erosion surfaces: In situ nuclide production. *Earth and Planetary Science Letters*, 104(2–4), 424–439. [https://doi.org/10.1016/0012-821x\(91\)90220-c](https://doi.org/10.1016/0012-821x(91)90220-c)
- Lal, R., Tims, S. G., Fifield, L. K., Wasson, R. J., & Howe, D. (2013). Applicability of ^{239}Pu as a tracer for soil erosion in the wet-dry tropics of northern Australia. *Nuclear Instruments and Methods in Physics Research Section B*, 294, 577–583. <https://doi.org/10.1016/j.nimb.2012.07.041>
- Leprun, J. C. (1994). Effets de la mise en valeur sur la dégradation physique des sols—Bilan du ruissellement et de l'érosion de quelques grands écosystèmes brésiliens. *Études et Gestion des sols*, 1, 45–65.
- Leprun, J. C., & Brossard, M. (2000). Balanço das medidas de perdas em terra e água por erosão hídrica em solos cultivados do Cerrado. O papel das pastagens. In *International symposium (2000/10/16-20), soil functioning under pastures in intertropical areas: Extended abstracts. Brasilia (BRA)* (Vol. 2000, 2p). EMBRAPA, IRD.
- Le Tourneau, F. M. (2019). Histoire, Géographie, Environnement. CNRS Éditions. L'Amazonie.
- Lifton, N., Caffee, M., Finkel, R., Marrero, S., Nishiizumi, K., Phillips, F. M., et al. (2015). In situ cosmogenic nuclide production rate calibration for the CRONUS-Earth project from Lake Bonneville, Utah, shoreline features. *Quaternary Geochronology*, 26, 56–69. <https://doi.org/10.1016/j.quageo.2014.11.002>
- Loba, A., Waroszewski, J., Sykula, M., Kabala, C., & Egli, M. (2022). Meteoric ^{10}Be , ^{137}Cs and $^{239+240}\text{Pu}$ as tracers of long- and medium-term soil erosion—A review. *Minerals*, 12(3), 359. <https://doi.org/10.3390/min12030359>
- Londero, A. L., Minella, J. P., Schneider, F. J., Deuschle, D., Merten, G. H., Evrard, O., & Boeni, M. (2021). Quantifying the impact of no-till on sediment yield in southern Brazil at the hillslope and catchment scales. *Hydrological Processes*, 35(7), e14286. <https://doi.org/10.1002/hyp.14286>
- Ludwig, W., Probst, J.-L., & Kempe, S. (1996). Predicting the oceanic input of organic carbon by continental erosion. *Global Biogeochemical Cycles*, 10(1), 23–41. <https://doi.org/10.1029/95GB02925>
- Mabit, L., Benmansour, M., & Walling, D. E. (2008). Comparative advantages and limitations of the fallout radionuclides ^{137}Cs , $^{210}\text{Pb}_{\text{ex}}$ and ^7Be for assessing soil erosion and sedimentation. *Journal of Environmental Radioactivity*, 99(12), 1799–1807. <https://doi.org/10.1016/j.jenvrad.2008.08.009>
- Mapbiomas (2022). Relatório Anual de Desmatamento 2021—São Paulo, Brasil MapBiomas.—126 páginas. <http://alerta.mapbiomas.org>
- Margulis, S., Dubeux, C. B. S., & Marcovitch, J. (2011). *The economics of climate change in Brazil: Costs and opportunities*. FEA/USP.
- Mathews, J. H., & Fink, K. D. (2004). *Numerical methods using MATLAB* (Vol. 4). Pearson Prentice Hall.
- Meybeck, M., & Vörösmarty, C. (2005). Fluvial filtering of land-to-ocean fluxes: From natural Holocene variations to Anthropocene. *Comptes Rendus Geoscience*, 337(1–2), 107–123. <https://doi.org/10.1016/j.crte.2004.09.016>
- Moreira, M. L. O., Moreton, L. C., Araújo, V. A. D., Lacerda Filho, J. V. D., & Costa, H. F. D. (2008). Geologia do Estado de Goiás e Distrito Federal. CPRM; SIC-FUNMINERAL.
- Norton, K. P., & Schlunegger, F. (2017). Lack of a weathering signal with increased Cenozoic erosion? *Terra Nova*, 29(5), 265–272. <https://doi.org/10.1111/ter.12278>
- Oliveira Filho, A. T., Sheperd, G. J., Martins, F. R., & Stubbleline, W. H. (1989). Environmental factors affecting physiognomy and floristic variation in an area of Cerrado in central Brazil. *Journal of Tropical Ecology*, 5(4), 413–431. <https://doi.org/10.1017/s0266467400003862>
- Ouimet, W. B., Whipple, K. X., & Granger, D. E. (2009). Beyond threshold hillslopes: Channel adjustment to base-level fall in tectonically active mountain ranges. *Geology*, 37(7), 579–582. <https://doi.org/10.1130/g30013a.1>
- Paisani, C. J., Pontelli, M. E., Corrêa, A. C. B., & Rodrigues, R. A. R. (2013). Pedogeochemistry and micromorphology of oxisols—A basis for understanding etchplanation in the Araucárias plateau (southern Brazil) in the late Quaternary. *Journal of South American Earth Sciences*, 48, 1–12. <https://doi.org/10.1016/j.jsames.2013.07.011>
- Pavich, M. J., Brown, L., Harden, J., Klein, J., & Middleton, R. (1986). ^{10}Be distribution in soils from Merced River terraces, California. *Geochimica et Cosmochimica Acta*, 50(8), 1727–1735. [https://doi.org/10.1016/0016-7037\(86\)90134-1](https://doi.org/10.1016/0016-7037(86)90134-1)
- Pennington, R. T., & Ratter, J. A. (2006). An overview of the plant diversity, biogeography and conservation of neotropical savannas and seasonally dry forests. In *Neotropical savannas and seasonally dry forests* (pp. 1–29). CRC Press.
- Pereira, A., Oliveira, S., Pereira, J., & Turkman, A. (2014). Modelling fire frequency in a cerrado savanna protected area. *PLoS One*, 9(7), e102380. <https://doi.org/10.1371/journal.pone.0102380>
- Persson, L., Carney Almroth, B. M., Collins, C. D., Cornell, S., de Wit, C. A., Diamond, M. L., et al. (2022). Outside the safe operating space of the planetary boundary for novel entities. *Environmental Science & Technology*, 56(3), 1510–1521. <https://doi.org/10.1021/acs.est.1c04158>
- Pimentel, D., & Burgess, M. (2013). Soil erosion threatens food production. *Agriculture*, 3(3), 443–463. <https://doi.org/10.3390/agriculture3030443>

- Poesen, J. (2018). Soil erosion in the Anthropocene: Research needs. *Earth Surface Processes and Landforms*, 43(1), 64–84. <https://doi.org/10.1002/esp.4250>
- Portenga, E. W., & Bierman, P. R. (2011). Understanding Earth's eroding surface with ^{10}Be . *Geological Society of America Today*, 21(8), 4–10. <https://doi.org/10.1130/g111a.1>
- Pupim, D. N. F., Bierman, P. R., Assine, M. L., Rood, D. H., Silva, A., & Merino, E. R. (2015). Erosion rates and landscape evolution of the lowlands of the Upper Paraguay river basin (Brazil) from cosmogenic ^{10}Be . *Geomorphology*, 234, 151–160. <https://doi.org/10.1016/j.geomorph.2015.01.016>
- Reatto, A., Martins, É. D. S., Farias, M. F. R., Silva, A. V. D., & Carvalho Júnior, O. A. D. (2004). Mapa pedológico digital-SIG atualizado do distrito federal escala 1: 100.000 e uma síntese do texto explicativo. *Embrapa Cerrados*.
- Renard, K. G., Foster, G. R., Weesies, G. A., & McCool, D. K. (1991). *Predicting soil erosion by water—A guide to conservation planning with the revised universal soil loss equation (RUSLE)*. Report ARS-703. Agricultural Research Service, US Department of Agriculture.
- Renard, K. G., Foster, G. R., Weesies, G. A., McCool, D. K., & Yoder, D. C. (1997). *Predicting soil erosion by water: A guide to conservation planning with the revised universal soil loss equation (RUSLE)* (p. 404). U.S. Department of Agriculture. Agriculture Handbook No. 703.
- Renard, K. G., Yoder, D. C., Lightle, D. T., & Dabney, S. M. (2011). Universal soil loss equation and revised universal soil loss equation. *Handbook of Erosion Modelling*, 8, 135–167.
- Reusser, L., Bierman, P., & Rood, D. (2015). Quantifying human impacts on rates of erosion and sediment transport at a landscape scale. *Geology*, 43(2), 171–174. <https://doi.org/10.1130/g36272.1>
- Reuter, H. I., Nelson, A., & Jarvis, A. (2007). An evaluation of void-filling interpolation methods for SRTM data. *International Journal of Geographical Information Science*, 21(9), 983–1008. <https://doi.org/10.1080/13658810601169899>
- Ribeiro, J. F., & Walter, B. M. T. (2008). As principais fitofisionomias do bioma cerrado. *Cerrado: Ecologia e Flora*, 1, 151–212.
- Righi, C. A., de Oliveira Risante, A. P., Packer, A. P., & do Couto, H. T. Z. (2023). Biodiversity and biomass relationships in a *cerrado stricto sensu* in Southeastern Brazil. *Environmental Monitoring and Assessment*, 195(4), 492. <https://doi.org/10.1007/s10661-023-11051-w>
- Ritchie, J. C., & McHenry, J. R. (1990). Application of radioactive fallout cesium-137 for measuring soil erosion and sediment accumulation rates and patterns: A review. *Journal of Environmental Quality*, 19(2), 215–233. <https://doi.org/10.2134/jeq1990.00472425001900020006x>
- Rochedo, P. R., Soares-Filho, B., Schaeffer, R., Viola, E., Szklo, A. F. P., Lucena, A. F. P., et al. (2018). The threat of political bargaining to climate mitigation in Brazil. *Nature Climate Change*, 8(8), 695–698. <https://doi.org/10.1038/s41558-018-0213-y>
- Rockström, J., Steffen, W., Noone, K., Persson, Å., Chapin, A. S., Lambin, E. F., et al. (2009). A safe operating space for humanity. *Nature*, 461(7263), 472–475. <https://doi.org/10.1038/461472a>
- Rosa, L. E., Cherem, L. F. S., & Soares, L. (2023). O papel de fatores naturais e antrópicos na variabilidade da perda de solos no estado de Goiás entre 1985 e 2018. *Sociedade & Natureza*, 35(1), e66034. <https://doi.org/10.14393/sn-v35-2023-66034>
- Ruddiman, W. F. (2003). The anthropogenic greenhouse era began thousands of years ago. *Climatic Change*, 61(3), 261–293. <https://doi.org/10.1023/b:clim.0000004577.17928.fa>
- Ruddiman, W. F. (2007). The early anthropogenic hypothesis: Challenges and responses. *Reviews of Geophysics*, 45, RG4001. <https://doi.org/10.1029/2006RG000207>
- Ruddiman, W. F. (2013). The Anthropocene. *Annual Review of Earth and Planetary Sciences*, 41(1), 45–68. <https://doi.org/10.1146/annurev-earth-050212-123944>
- Salgado, A. A. R., Braucher, R., Varajao, A. C., Colin, F., Varajao, A. F. D. C., & Nalini, H. A., Jr. (2008). Relief evolution of the Quadrilátero Ferrífero (Minas Gerais, Brazil) by means of [^{10}Be] cosmogenic nuclei. *Zeitschrift für Geomorphologie*, 52(3), 317–323. <https://doi.org/10.1127/0372-8854/2008/0052-0317>
- Salgado, A. A. R., de Andrade Rezende, E., Bourlès, D., Braucher, R., da Silva, J. R., & Garcia, R. A. (2016). Relief evolution of the Continental Rift of Southeast Brazil revealed by in situ-produced ^{10}Be concentrations in river-borne sediments. *Journal of South American Earth Sciences*, 67, 89–99. <https://doi.org/10.1016/j.jsames.2016.02.002>
- Schäfer, J. M., Ivy-Ochs, S., Wieler, R., Leya, I., Baur, H., Denton, G. H., & Schlüchter, C. (1999). Cosmogenic noble gas studies in the oldest landscape on earth: Surface exposure ages of the dry valleys, Antarctica. *Earth and Planetary Science Letters*, 167(3–4), 215–226. [https://doi.org/10.1016/s0012-821x\(99\)00029-1](https://doi.org/10.1016/s0012-821x(99)00029-1)
- Schmidt, A. H., Neilson, T. B., Bierman, P. R., Rood, D. H., Ouimet, W. B., & Sosa Gonzalez, V. (2016). Influence of topography and human activity on apparent in situ ^{10}Be -derived erosion rates in Yunnan, SW China. *Earth Surface Dynamics*, 4(4), 819–830. <https://doi.org/10.5194/esurf-4-819-2016>
- Scholes, R. J., Montanarella, L., Brainich, E., Barger, N., Ten Brink, B., Cantele, M., et al. (2018). Ipbes (2018): Summary for policymakers of the assessment report on land degradation and restoration of the Intergovernmental Science-Policy Platform on Biodiversity and Ecosystem Services (44p).
- Schoonejans, J., Vanacker, V., Opfergelt, S., & Christl, M. (2017). Long-term soil erosion derived from in-situ ^{10}Be and inventories of meteoric ^{10}Be in deeply weathered soils in southern Brazil. *Chemical Geology*, 466, 380–388. <https://doi.org/10.1016/j.chemgeo.2017.06.025>
- Shuster, D. L., Farley, K. A., Vasconcelos, P. M., Balco, G., Monteiro, H. S., Waltenberg, K., & Stone, J. O. (2012). Cosmogenic ^3He in hematite and goethite from Brazilian “canga” duricrust demonstrates the extreme stability of these surfaces. *Earth and Planetary Science Letters*, 329, 41–50. <https://doi.org/10.1016/j.epsl.2012.02.017>
- Siame, L., Rosa, L., Cherem, L. F., Oliveira, J., Evrard, O., Barhoumi, H., et al. (2023). Data and supplementary information for “Natural versus anthropogenic erosion in Central Brazil, a confrontation of time and space scales” (VERSION 1) Dataset]. DataSuds. <https://doi.org/10.23708/U65XXY>
- Siame, L. L., Angelier, J., Chen, R.-F., Godard, V., Derriex, F., Bourlès, D. L., et al. (2011). Erosion rates in an active orogen (NE-Taiwan): Erosion rates in an active orogen (NE-Taiwan): A confrontation of cosmogenic measurements with river suspended loads. *Quaternary Geochronology*, 6(2), 246–260. <https://doi.org/10.1016/j.quageo.2010.11.003>
- Sordi, M. V., Salgado, A. A. R., Siame, L., Bourlès, D., Paisani, J. C., Leanni, L., et al. (2018). Implications of drainage rearrangement for passive margin escarpment evolution in Southern Brazil. *Geomorphology*, 306, 155–169. <https://doi.org/10.1016/j.geomorph.2018.01.007>
- Steffen, W., Richardson, K., Rockström, J., Cornell, S. E., Fetzer, I., Bennett, E. M., et al. (2015). Planetary boundaries: Guiding human development on a changing planet. *Science*, 347(6223), 1259855. <https://doi.org/10.1126/science.1259855>
- Steffen, W., Rockström, J., Richardson, K., Lenton, T. M., Folke, C., Liverman, D., et al. (2018). Trajectories of the earth system in the Anthropocene. *Proceedings of the National Academy of Sciences of the United States of America*, 115(33), 8252–8259. <https://doi.org/10.1073/pnas.1810141115>
- Stone, J. O. (2000). Air pressure and cosmogenic isotope production. *Journal of Geophysical Research*, 105(B10), 23753–23759. <https://doi.org/10.1029/2000JB900181>

- Strassburg, B. B., Brooks, T., Feltran-Barbieri, R., Iribarrem, A., Crouzeilles, R., Loyola, R., et al. (2017). Moment of truth for the Cerrado hotspot. *Nature Ecology & Evolution*, 1(4), 0099. <https://doi.org/10.1038/s41559-017-0099>
- Summerfield, M., & Hulton, N. (1994). Natural controls of fluvial denudation rates in major world drainage basins. *Journal of Geophysical Research*, 99(B7), 13871–13883. <https://doi.org/10.1029/94JB00715>
- Syvitski, J. P., & Milliman, J. D. (2007). Geology, geography, and humans battle for dominance over the delivery of fluvial sediment to the coastal ocean. *The Journal of Geology*, 115(1), 1–19. <https://doi.org/10.1086/509246>
- Syvitski, J. P., Vörösmarty, C. J., Kettner, A. J., & Green, P. (2005). Impact of humans on the flux of terrestrial sediment to the global coastal ocean. *Science*, 308(5720), 376–380. <https://doi.org/10.1126/science.1109454>
- Takahashi, Y., Minai, Y., Ambe, S., Makide, Y., & Ambe, F. (1999). Comparison of adsorption behavior of multiple inorganic ions on kaolinite and silica in the presence of humic acid using the multitracer technique. *Geochimica et Cosmochimica Acta*, 63(6), 815–836. [https://doi.org/10.1016/S0016-7037\(99\)00065-4](https://doi.org/10.1016/S0016-7037(99)00065-4)
- Turner, B., Clark, W., Kates, R., Richards, J., Mathews, J., & Meyer, W. (1990). The earth as transformed by human action: Global change and regional changes in the biosphere over the past 300 years. In *The earth as transformed by human action: Global change and regional changes in the biosphere over the past 300 years*. Cambridge University Press, with Clark University.
- Vanacker, V., Ameijeiras-Mariño, Y., Schoonejans, J., Cornélis, J. T., Minella, J. P., Lamouline, F., et al. (2019). Land use impacts on soil erosion and rejuvenation in Southern Brazil. *Catena*, 178, 256–266. <https://doi.org/10.1016/j.catena.2019.03.024>
- Vanacker, V., Bellin, N., Molina, A., & Kubik, P. W. (2014). Erosion regulation as a function of human disturbances to vegetation cover: A conceptual model. *Landscape Ecology*, 29(2), 293–309. <https://doi.org/10.1007/s10980-013-9956-z>
- Vanacker, V., von Blanckenburg, F., Govers, G., Molina, A., Poesen, J., Deckers, J., & Kubik, P. (2007). Restoring dense vegetation can slow mountain erosion to near natural benchmark levels. *Geology*, 35(4), 303–306. <https://doi.org/10.1130/g23109a.1>
- Van Oost, K., Quine, T. A., Govers, G., De Gryze, S., Six, J., Harden, J. W., et al. (2007). The impact of agricultural soil erosion on the global carbon cycle. *Science*, 318(5850), 626–629. <https://doi.org/10.1126/science.1145724>
- Varajão, C. A. C., de Alkmim, F. F., Braucher, R., Endo, I., Cherem, L. F. S., Salgado, A. A. R., & Varajão, A. F. D. C. (2018). Denudation rates in the Pancas Bornhardt Province (SE Brazil), inferred from in situ produced cosmogenic ¹⁰Be. *Zeitschrift für Geomorphologie*, 62(1), 13–22. <https://doi.org/10.1127/zfg/2018/0496>
- Vasconcelos, P. M., Farley, K. A., Stone, J., Piacentini, T., & Fifield, L. K. (2019). Stranded landscapes in the humid tropics: Earth's oldest land surfaces. *Earth and Planetary Science Letters*, 519, 152–164. <https://doi.org/10.1016/j.epsl.2019.04.014>
- Vesely, J., Norton, S. A., Skrivan, P., Majer, V., Kram, P., Navratil, T., & Kaste, J. M. (2002). Environmental chemistry of beryllium. *Reviews in Mineralogy and Geochemistry*, 50(1), 291–317. <https://doi.org/10.2138/rmg.2002.50.7>
- von Blanckenburg, F. (2005). The control mechanisms of erosion and weathering at basin scale from cosmogenic nuclides in river sediment. *Earth and Planetary Science Letters*, 237(3–4), 462–479. <https://doi.org/10.1016/j.epsl.2005.06.030>
- von Blanckenburg, F., Bouchez, J., & Wittmann, H. (2012). Earth surface erosion and weathering from the ¹⁰Be (meteoric)/⁹Be ratio. *Earth and Planetary Science Letters*, 351, 295–305. <https://doi.org/10.1016/j.epsl.2012.07.022>
- Walling, D. E., & He, Q. (1997). *Models for converting 137Cs measurements to estimates of soil redistribution rates on cultivated and uncultivated soils (including software for model implementation)*. Report to IAEA (p. 315e341). University of Exeter.
- Walling, D. E., He, Q., & Appleby, P. G. (2002). Conversion models for use in soil-erosion, soil-redistribution and sedimentation investigations. In F. Zapata (Ed.), *Handbook for the assessment of soil erosion and sedimentation using environmental radionuclides* (pp. 111–164). Kluwer.
- Walling, D. E., & Quine, T. A. (1990). Calibration of caesium-137 measurements to provide quantitative erosion rate data. *Land Degradation & Development*, 2(3), 161–175. <https://doi.org/10.1002/ldr.3400020302>
- Wang-Erlandsson, L., Tobian, A., van der Ent, R. J., Fetzer, I., te Wierik, S., Porkka, M., et al. (2022). A planetary boundary for green water. *Nature Reviews Earth & Environment*, 3(6), 380–392. <https://doi.org/10.1038/s43017-022-00287-8>
- West, N., Kirby, E., Bierman, P., Slingerland, R., Ma, L., Rood, D., & Brantley, S. (2013). Regolith production and transport at the Susquehanna Shale Hills critical zone observatory, Part 2: Insights from meteoric ¹⁰Be. *Journal of Geophysical Research: Earth Surface*, 118, 1877–1896. <https://doi.org/10.1002/jgrf.20121>
- Wilkinson, B. H. (2005). Humans as geologic agents: A deep-time perspective. *Geology*, 33(3), 161–164. <https://doi.org/10.1130/g21108.1>
- Wilkinson, B. H., & McElroy, B. J. (2007). The impact of humans on continental erosion and sedimentation. *Geological Society of America Bulletin*, 119(1–2), 140–156. <https://doi.org/10.1130/b25899.1>
- Willenbring, J. K., & Jerolmack, D. J. (2016). The null hypothesis: Globally steady rates of erosion, weathering fluxes and shelf sediment accumulation during late Cenozoic mountain uplift and glaciation. *Terra Nova*, 28(1), 11–18. <https://doi.org/10.1111/ter.12185>
- Willenbring, J. K., & von Blanckenburg, F. (2010). Meteoric cosmogenic Beryllium-10 adsorbed to river sediment and soil: Applications for Earth-surface dynamics. *Earth-Science Reviews*, 98(1–2), 105–122. <https://doi.org/10.1016/j.earscirev.2009.10.008>
- Winkler, K., Fuchs, R., Rounsevell, M., & Herold, M. (2021). Global land use changes are four times greater than previously estimated. *Nature Communications*, 12(1), 2501. <https://doi.org/10.1038/s41467-021-22702-2>
- Wittmann, H., Oelze, M., Roig, H., & von Blanckenburg, F. (2018). Are seasonal variations in river-floodplain sediment exchange in the lower Amazon River basin resolvable through meteoric cosmogenic ¹⁰Be to stable ⁹Be ratios? *Geomorphology*, 322, 148–158. <https://doi.org/10.1016/j.geomorph.2018.08.045>
- Wittmann, H., von Blanckenburg, F., Bouchez, J., Dannhaus, N., Naumann, R., Christl, M., & Gaillardet, J. (2012). The dependence of meteoric ¹⁰Be concentrations on particle size in Amazon Riverbed sediment and the extraction of reactive ¹⁰Be/⁹Be ratios. *Chemical Geology*, 318, 126–138. <https://doi.org/10.1016/j.chemgeo.2012.04.031>
- Wyshnytzky, C. E., Ouimet, W. B., McCarthy, J., Dethier, D. P., Shroba, R. R., Bierman, P. R., & Rood, D. H. (2015). Meteoric ¹⁰Be, clay, and extractable iron depth profiles in the Colorado Front Range: Implications for understanding soil mixing and erosion. *Catena*, 127, 32–45. <https://doi.org/10.1016/j.catena.2014.12.008>
- Xiong, M., Sun, R., & Chen, L. (2019). A global comparison of soil erosion associated with land use and climate type. *Geoderma*, 343, 31–39. <https://doi.org/10.1016/j.geoderma.2019.02.013>
- You, C.-F., Lee, T., & Li, Y.-H. (1989). The partition of Be between soil and water. *Chemical Geology*, 77(2), 105–118. [https://doi.org/10.1016/0009-2541\(89\)90136-8](https://doi.org/10.1016/0009-2541(89)90136-8)
- Zalles, V., Hansen, M. C., Potapov, P. V., Stehman, S. V., Tyukavina, A., Pickens, A., et al. (2019). Near doubling of Brazil's intensive row crop area since 2000. *Proceedings of the National Academy of Sciences of the United States of America*, 116(2), 428–435. <https://doi.org/10.1073/pnas.1810301115>
- Zapata, F. (Ed.). (2002). *Handbook for the assessment of soil erosion and sedimentation using environmental radionuclides* (Vol. 219). Kluwer Academic Publishers.